JPET Fast Forward. Published on October 5, 2005 as DOI: 10.1124/jpet.105.094326

Protective Effect of Type 2 Diabetes on Acetaminophen-induced Hepatotoxicity in Male Swiss Webster Mice

Sharmilee P. Sawant, Ankur V. Dnyanmote, Mayurranjan S. Mitra, Jaya Chilakapati, Alan Warbritton, John R. Latendresse, and Harihara M. Mehendale

Department of Toxicology, College of Pharmacy, The University of Louisiana Monroe, Monroe, LA, USA (S.P.S., A.V.D., M.S.M., J.C., H.M.M.); Toxicologic Pathology Associates, National Center for Toxicological Research, Jefferson, AR, USA (A.W., J.R.L.)

JPET Fast Forward. Published on October 5, 2005 as DOI: 10.1124/jpet.105.094326
This article has not been copyedited and formatted. The final version may differ from this version.

A) **Running Title:** Acetaminophen Hepatotoxicity in Type 2 Diabetic Mice

B) Address correspondence to:

Harihara M. Mehendale, Ph.D.,

Department of Toxicology, College of Pharmacy, The University of Louisiana Monroe, 700 University Avenue, Monroe, LA 71209-0470, USA.

Phone: 318-342-1691, Fax: 318-342-1686

E-mail: mehendale@ulm.edu

C)

Number of Text Pages	**:** 45
Number of Tables	**:** 2
Number of Figures	**:** 10
Number of References	**:** 40
Number of Words in the Abstract	**:** 250
Number of Words in the Introduction	**:** 835
Number of Words in the Discussion	**:** 2235

D) ABBREVIATIONS: APAP, acetaminophen; APAP-G, acetaminophen glucuronide; ALT, alanine aminotransferase; AST, aspartate aminotransferase; BB, bromobenzene; BSA, bovine serum albumin; CLC, colchicine; CYP P450, cytochrome P450; DAB, diaminobenzidine; DB, diabetic; DW, distilled water; GSH, glutathione; H&E, hematoxylin and eosin; HFD, high fat diet fed rats injected citrate buffer; HFD + STZ, high fat diet fed rats injected streptozotocin; HRP, horseradish peroxidase; [^{3}H]-T, tritiated thymidine; NAPQI, *N*-acetyl-*p*-benzoquinoneimine; ND, normal diet fed rats injected citrate buffer; non-DB, non-diabetic; ND + STZ, normal diet fed rats injected streptozotocin; ob/ob, C57 BL/6J obese mice; PCNA, proliferating cell nuclear antigen; PNP, para-nitrophenol; PPAR-α, peroxisome proliferator activated receptor-alpha; SD, Sprague Dawley; SDS, sodium dodecyl sulphate; STZ, streptozotocin; SW, Swiss Webster; TA, thioacetamide; TCA, trichloroacetic acid.

E) Recommended Section Assignment: Toxicology

JPET Fast Forward. Published on October 5, 2005 as DOI: 10.1124/jpet.105.094326
This article has not been copyedited and formatted. The final version may differ from this version.

ABSTRACT

Type 2 diabetic (DB) mice exposed to CCl_4 (LD_{50}, 1.25 ml/kg), acetaminophen (LD_{80}, 600 mg/kg, APAP), and bromobenzene (LD_{80}, 0.5 ml/kg), ip, yielded 30, 20, and 20% mortality, respectively, indicating hepatotoxic resistance. Male Swiss Webster mice were made diabetic by feeding high fat and administrating streptozotocin (120 mg/kg, ip) on day 60. On day 71, time course studies after APAP (600 mg/kg) treatment revealed identical initial liver injury in non-DB and DB mice, which progressed only in non-DB mice resulting in 80% mortality. The hypothesis that decreased APAP bioactivation, altered toxicokinetics, and/or increased tissue repair are the underlying mechanisms was investigated. HPLC analysis revealed no change in plasma and urinary APAP, detoxification of APAP via glucuronidation between DB and non-DB mice. Hepatic CYP2E1 protein and activity, glutathione, and ^{14}C-APAP covalent binding did not differ between DB and non-DB mice, suggesting that lower bioactivation-based injury is not the mechanism of decreased hepatotoxicity in DB mice. Diabetes increased cells in S-phase by 8-fold in normally quiescent liver of these mice. Immunohistochemistry revealed over-expression of calpastatin, in the newly dividing/divided cells explaining inhibition of hydrolytic enzyme, calpain, in perinecrotic areas and lower progression of APAP-initiated injury in the DB mice. Antimitotic intervention of diabetes-associated cell division with colchicine before APAP administration resulted in 70% mortality in APAP treated CLC intervened DB mice. These studies suggest that advancement of cells in the cell division cycle and higher tissue repair protect DB mice by preventing progression of APAP-initiated liver injury that normally leads to mortality.

Introduction

An epidemiological study showed that diabetic (DB) patients are nearly twice as likely to suffer from hepatic failure compared to non-DB patients (El-Serag and Everhart, 2002). Several studies conducted in type 1 DB rats and mice to test hepatotoxic sensitivity clearly indicate that type 1 DB rats are sensitive (El-Hawari and Plaa, 1983; Grant and Duthie, 1988; Watkins et al., 1988; Wang et al., 2000a) while the type 1 DB mice are resistant to hepatotoxicity induced by several dissimilar hepatotoxicants (Shankar et al., 2003a; Shankar et al., 2003c), indicating species difference in hepatotoxic sensitivity. Studies by Wang et al. (2000a; 2000b; 2001) in type 1 DB rats indicated that inhibited compensatory tissue repair plays a determining role in the final toxic outcome following thioacetamide (TA) administration. In stark contrast, type 1 DB mice challenged with TA and acetaminophen (APAP) exhibit higher hepatic tissue repair (Shankar et al., 2003a) and higher renal tissue repair after challenge with 1,2, dichlorovinyl-L-cysteine (Dnyanmote et al., 2005). It is known that hepatoprotection in type 1 DB mice is dependent on PPAR-α activation (Shankar et al., 2003b).

Very few studies have investigated the effect of type 2 diabetes on hepatotoxic sensitivity, even though it is the most prevalent form of diabetes, representing 90-95% of the DB population. One reason is the lack of a robust and well-characterized type 2 DB rodent model. Disadvantages of most commonly used genetic models are transient and moderate hyperglycemia (3 to 5 months of age), lack of insulin resistance, and extreme degree of hyperinsulinemia (Bailey and Flatt, 1991; Portha et al., 1991). Recently, Sawant and coworkers (2004) have refined and characterized a non-obese type 2 diabetes rat model based on high fat diet and a low dose of streptozotocin. Using 12 different parameters, Sawant et al. (2004) reported that these DB rats closely resemble type 2 DB patients. Their studies revealed for the first time that type 2 DB rats are sensitive to structurally and mechanistically

different hepatotoxicants (Sawant et al., 2004), similar to type 1 DB rats. Time course studies using two model hepatotoxicants, CCl_4 and TA, showed that CCl_4- and TA-hepatotoxicity is potentiated in type 2 DB rats not due to increased bioactivation-based mechanisms but due to inhibited compensatory tissue repair response (Sawant et al., 2004; Sawant et al., 2005).

Whether there is species difference in hepatotoxic sensitivity due to type 2 diabetes similar to that observed in type 1 DB rats and mice is not known. Therefore, the objectives of the present study were to evaluate hepatotoxic sensitivity of type 2 DB mice to three dissimilar hepatotoxicants including APAP and investigate the mechanisms of hepatotoxic resistance.

APAP remains the commonest cause of acute liver failure in the United States and other parts of the world as a result of accidental or deliberate overdose (Dargan and Jones, 2003). Several mechanisms have been shown to protect from APAP hepatotoxicity such as inhibition of cytochrome P450s (Mitchell et al., 1973; Zaher et al., 1998); enhanced detoxification via glucuronidation of APAP (Hazelton et al., 1986); treatment with N-acetylcysteine, repletion of GSH or enhanced antioxidant status (Corcoran et al., 1985; Jaeschke, 1990); inhibition of hydrolytic enzymes such as calpain by treatment with synthetic calpain inhibitor or over-expression of its endogenous inhibitor, calpastatin (Limaye et al., 2003; Limaye et al., 2005); and by stimulated cell division and liver tissue repair (Shankar et al., 2003a; Shankar et al., 2003b).

Using APAP, CCl_4, and bromobenzene (BB) as model hepatotoxicants, we tested the hypothesis that type 2 DB mice exhibit hepatotoxic resistance. The specific aims of the present study were to investigate whether protection from APAP-induced hepatotoxicity in the DB mice is due to: (1) decreased bioactivation via decreased CYP2E1 and decreased covalent binding of ^{14}C-APAP-derived radiolabel to liver macromolecules; (2) increased detoxification via nontoxic APAP-glucuronidation and glutathione conjugation; (3) advancement of liver cells to S-phase in type 2 DB mice, unlike the quiescent non-DB mice,

protecting DB mice from expansion of APAP-initiated liver injury; (4) over-expression of calpastatin in dividing or newly divided cells resulting in decreased progression of liver injury via inhibited calpain after exposure to APAP. Finally, to test whether or not diabetes-related advancement of liver cells to S-phase is critical for hepatoprotection, DB mice received colchicine (CLC) intervention before the administration of APAP.

We report here that unlike the type 2 DB rats, the type 2 DB mice are resistant to three dissimilar hepatotoxicants. The resistance of type 2 DB mice against APAP-hepatotoxicity appears to be neither due to decreased bioactivation nor due to altered toxicokinetics but because of diabetes-associated 8-fold advancement of hepatocytes to S-phase, which prevents progression of APAP-initiated injury while facilitating restoration of liver structure and function via early onset of robust tissue repair. Inhibition of this entry into S-phase of cell division by CLC intervention abolished the hepatoprotection in the DB mice, which lends further credence to the notion that diabetes-related advancement of cells in cell division cycle and higher tissue repair are pivotal to the protection of type 2 DB mice from APAP-hepatotoxicity.

JPET Fast Forward. Published on October 5, 2005 as DOI: 10.1124/jpet.105.094326
This article has not been copyedited and formatted. The final version may differ from this version.

Materials and Methods

Animals and Diets

Male Swiss Webster (SW) mice (25–30 g) were obtained from Harlan Sprague Dawley (Indianapolis, IN). They were housed over sawdust bedding (Sani-Chips®, Harlan Teklad, Madison, WI) in a controlled environment (temperature 21 ± 1^{o}C, humidity 50 ± 10%, and 12:12 h light: dark cycle) and were acclimatized for a week before use in experiments. Mice had free access to water and rodent chow [normal rodent diet consisting of 6% fat, 20% protein, and 53% carbohydrate (Harlan Teklad, Rat Chow # 7012, Madison, WI); or high fat diet consisting of 20% fat, 20% protein, and 46% carbohydrate (Dyets Inc., Dyets # 100795, Bethlehem, PA)]. Animal maintenance and treatment were in accordance with the National Institute of Health Guide for Laboratory Animal Welfare, as approved by our Institutional Animal Care and Use Committee (IACUC).

Chemicals

Unless stated otherwise, all chemicals and biochemical kits were purchased from Sigma Chemical Co. (St. Louis, MO) and ThermoDMA (Arlington, TX), respectively. [^{3}H-CH_3]-Thymidine ([^{3}H]-T, 2 Ci/mmol) was purchased from Moravek Biochemicals Inc. (Brea, CA); scintillation fluid was obtained from Fisher Scientific Co. (Baton Rouge, LA).

Treatments

Induction of Type 2 Diabetes. The experimental protocol described previously (Sawant et al., 2004) to induce type 2 diabetes in rats was employed to induce diabetes in mice. Preliminary studies established that induction of type 2 diabetes in mice required longer duration of feeding high fat diet. SW mice were fed high fat diet for 60 days unlike the two week protocol for SD rats. Beginning on day 0, mice were fed either normal rodent chow or

JPET Fast Forward. Published on October 5, 2005 as DOI: 10.1124/jpet.105.094326
This article has not been copyedited and formatted. The final version may differ from this version.

high fat diet. On day 60, mice on the high fat diet were injected with either a single dose of streptozotocin (STZ, 120 mg/kg, ip, in 0.01 M citrate buffer, pH 4.3, HFD + STZ group) to induce diabetes or citrate buffer (10 ml/kg, ip) (HFD) to serve as vehicle control. Mice on the normal rodent diet injected with either a single dose of STZ (120 mg/kg, ip, in 0.01 M citrate buffer, pH 4.3) (ND + STZ) or citrate buffer (10 ml/kg, ip) (ND) served as non-DB controls. Subsequent to STZ or citrate buffer treatment, mice had free access to food and water and were continued on their respective diets for the entire duration of study. Blood sampled from the retro orbital plexus under diethyl ether anesthesia on day 70 was used to measure plasma glucose and insulin concentrations. Mice exhibiting plasma glucose (400 ± 54 mg/dl) compared to the non-DB mice (ND, ND + STZ, HFD groups, 128 ± 10 mg/dl) (Sigma Kit no. 315-100) and plasma insulin in the normal range of 0.5 to 2 ng/ml (ELISA, Crystal Chem Co., Downers Grove, IL) were considered to have type 2 diabetes (HFD + STZ group). Thus, the HFD + STZ group represents the DB group. The three non-DB controls were ND, ND + STZ and HFD. This protocol routinely renders 90% of the mice maintained on high fat diet and given STZ, diabetic.

Characterization of Type 2 Diabetes Model

Glucose and Insulin Levels. On day 70 of the experimental protocol, in the DB mice (HFD + STZ group), type 2 diabetes was confirmed by measuring non-fasting plasma glucose and plasma insulin levels.

Oral Glucose Tolerance Test. To assess oral glucose tolerance, mice (n = 4 each group) were fasted overnight (12 h) and their plasma glucose response to oral administration of a bolus glucose solution (20% solution, 5 g/kg) was determined. Blood samples were taken from the retro orbital plexus under diethyl ether anesthesia before (time 0) and 2 h after glucose administration. Plasma glucose and insulin concentrations were estimated.

JPET Fast Forward. Published on October 5, 2005 as DOI: 10.1124/jpet.105.094326
This article has not been copyedited and formatted. The final version may differ from this version.

Lethality Study

On day 71 of the experimental protocol, DB (HFD + STZ group) and non-DB mice (ND, ND + STZ, HFD groups) (*n* = 10 per group) were treated with CCl_4 (1.25 ml/kg, ip, in 10 ml/kg corn oil) or corn oil (10 ml/kg, ip); acetaminophen (APAP, 600 mg/kg, ip, in warm basic saline, pH 8, 20 ml/kg) or vehicle control (warm basic saline, pH 8, 20 ml/kg); or bromobenzene (BB, 0.5 ml/kg, ip, in 10 ml of corn oil) or corn oil (10 ml/kg, ip). Survival and mortality were recorded thrice on the first day and twice daily thereafter for a total of 14 days.

APAP-induced Liver Injury. On day 71, DB (HFD + STZ group) and non-DB mice (ND, HFD, ND+STZ groups) were treated with either a single injection of APAP (600 mg/kg, ip, warm basic saline, pH 8, 20 ml/kg) or vehicle control (20 ml/kg, ip, warm basic saline, pH 8). The mice treated with APAP were terminated with diethyl ether for the time course studies (0 to 96 h). Four mice (n = 4) were treated per group per time point, except for non-DB groups (n = 20) treated with APAP, in order to obtain four surviving mice at 12, 24, 48, and 96 h after APAP administration.

The plasma and liver tissue from these mice were collected at 0, 6, 12, 24, 48, and 96 h after dosing. From the DB and non-DB mice treated with warm basic saline vehicle, blood and liver samples were collected only at 0, 12, and 24 h after saline administration (*n* = 4/group /time point).

Hepatotoxicity

Estimation of Liver Injury. Plasma was separated by heparinization and centrifugation. Plasma alanine aminotransferase (ALT) and aspartate aminotransferase (AST) were

measured as biomarkers of liver injury using ThermoDMA kit # TR 7111-125 and kit # TR 7011-125, respectively.

Histopathology. Portions of liver were taken from the left lateral lobes and fixed immediately in 10% phosphate-buffered formalin and after 48 h stored in 70% alcohol until further processing. The liver sections were processed, and then embedded in paraffin. Liver sections (5 μm thin) were stained with hematoxylin and eosin (H&E) for histological examination by light microscopy. Unstained liver sections were prepared for calpain, calpastatin, and proliferating cell nuclear antigen (PCNA) immunohistochemistry.

Effect of Type 2 Diabetes on Hepatic Microsomal CYP2E1 and Covalent Binding to Liver Macromolecules

Preparation of Microsomes. Liver microsomes were prepared by differential ultracentrifugation using the method described earlier (Chipman et al., 1979). Protein content of the microsomes was estimated by Bradford's method using the BioRad protein assay (BioRad Laboratories, CA). Microsomes were stored at –80^{o}C until needed.

CYP2E1 Western Blot Analysis. Liver microsomal protein (20 μg) from each mouse was separated by SDS-polyacrylamide gel electrophoresis and transferred to membranes (Wang et al., 2001). To detect CYP2E1 protein, nitrocellulose membranes (BioRad, Hercules, CA) were incubated with a primary goat anti-rat CYP2E1 polyclonal antibody (Gentest Inc., Woburn, MA). The blots were further incubated with anti-goat secondary antibody conjugated to horseradish peroxidase (HRP) and visualized using a chemiluminescence kit obtained from Pierce Biotechnology (Bradford, IL). Immunoquantification was carried out using a GS-700 imaging densitometer (BioRad, Hercules, CA) followed by quantitation using Quantity One software (BioRad, Hercules, CA).

CYP2E1 Enzyme Activity Assays. Microsomal CYP2E1-dependent hydroxylation of *p*-nitrophenol (PNP) to *p*-nitrocatechol was used as a standard assay to quantify CYP2E1 activity (Wang et al., 2001).

In vivo Covalent Binding of ^{14}C-APAP-derived Radiolabel to Liver Proteins. Covalent binding of ^{14}C-APAP-derived radiolabel to liver macromolecules was estimated in the non-DB (ND group only) and DB mice. Livers from ND and DB mice treated with ^{14}C-APAP (600 mg/kg, ip, 4.3 mCi/mmol, 5 μCi/mouse, Sigma Chemical Co., St. Louis, MO) were flash frozen at 2 h after APAP treatment. Covalently bound ^{14}C-APAP-derived label to liver macromolecules was estimated using procedure described by Shankar et al. (2003a). Briefly, liver tissue (200 mg) was homogenized in 1 ml of 0.9% saline and total protein precipitated using 2 ml of 0.9 M trichloroacetic acid (TCA). Samples were centrifuged at 1000 *g* for 15 min at room temperature. The supernatant was discarded and the precipitate was resuspended in 3 ml of 0.6 M TCA, mixed using a Vortex agitator, and centrifuged at 1000 *g* for 5 min. After 2 more washings with 0.6 M TCA, the pellet was washed eight times with 80% methanol (6 ml per wash) and the radioactivity in the methanol wash was estimated each time. After 8 methanol washings no radioactivity was detected in the supernatant. The pellets (containing covalently bound ^{14}C-APAP-derived radiolabel) were air-dried, dissolved in 2 ml 1 N NaOH, and an aliquot was used to estimate ^{14}C-APAP using a liquid scintillation counter and the protein concentrations were determined using a BioRad protein assay kit (BioRad, Hercules, CA). The results are expressed as DPM per mg liver protein.

Effect of Type 2 Diabetes in APAP Toxicokinetics

Toxicokinetic Parameters of APAP. Blood (50 μl) was collected from non-DB (ND group) and DB mice at 0, 5, 10, 15, 30, 45, 60, 120, 180, 240, 360, and 720 min after APAP

JPET Fast Forward. Published on October 5, 2005 as DOI: 10.1124/jpet.105.094326
This article has not been copyedited and formatted. The final version may differ from this version.

administration (600 mg/kg, ip). To complete the entire time course once (n = 1), three mice had to be used. Four time points were collected from each mouse overlapping one time point between mice. Three such replicate time courses (n=3) were performed for ND and DB mice. APAP and APAP-glucuronide (APAP-G) were estimated using a reverse-phase HPLC analysis using a SPS-ODS column (5 μm, Regis Technologies, Mortongrove, IL). In a separate study (n = 45 and 12 for ND and DB mice, respectively), urine was collected at 0, 12, and 24 h after APAP administration to ND and DB mice. For the estimation of plasma APAP and APAP-G and urinary APAP levels, 7% acetonitrile in Na-K-phosphate (50 mM) buffer (pH 7.4) was used as the mobile phase at a flow rate of 1 ml/min (Shankar et al., 2003a).

However, for the estimation of the urinary APAP-G, the urine samples were diluted with two volumes of ice-cold methanol (HPLC grade, Sigma Chemical Co., St. Louis, MO) and centrifuged at 1200 *g* for 30 min, 100 μl of the supernatant was used for HPLC analysis. The urinary APAP-G was estimated by HPLC analysis using an isocratic mobile phase of 12.5% methanol, 1% acetic acid, and 86.5% deionized water at a flow rate of 0.8 ml/min (Chen et al., 2003) using a reverse-phase column (SPS-ODS column, 5 μm, Regis Technologies, Mortongrove, IL).

APAP and APAP-G (HPLC grade, Sigma Chemical Co., St. Louis, MO) were used as standards. APAP-G and APAP were detected at 254 nm, with retention times of 2.6 and 8.1 min, respectively, using a PDA-100 photodiode array detector (Dionex Systems, Sunnyvale, CA). Plasma half-life ($t_{1/2}$) for APAP was computed using the elimination constant (β), where $t_{1/2} = 0.693/\beta$. The value of β was estimated using a semi logarithmic plot of time versus concentration (up to 360 min) using JMP-IN statistical software (SAS Institute, Cary, NC).

Glutathione Estimation. Total and reduced GSH was estimated in livers of non-DB (ND group) and DB mice challenged with APAP (600 mg/kg, ip) at 0, 2, and 6 h after APAP treatment. A commercially available kit (Cat# 703002) from Cayman Chemical Company (Ann Arbor, MI) was used. The kit is based on enzymatic recycling of GSH using GSH reductase followed by reaction of GSH with Ellman's reagent. Blue colored product was read at 405 nm and quantitated on a standard curve.

Progression and Regression of Injury: Calpain-Calpastatin System

Calpain and Calpastatin Immunohistochemistry. Calpain immunohistochemistry was conducted using method described previously (Limaye et al., 2003). Briefly, liver sections from the non-DB (ND group) and DB mice were deparaffinised and antigen retrival was achieved using citrate buffer (pH 6.0) for 8 min. The sections were blocked using 3% bovine serum albumin (BSA) for 1 h and incubated with polyclonal anti-rabbit primary calpain antibody (1:500, Sigma Chemical Co., St. Louis., MO) for 14 h at 4^{o}C. A HRP conjugated secondary anti-rabbit IgG antibody (1:500) was then linked to the primary antibody before incubation with diaminobenzidine (DAB), which gives a brown reaction product. The cells were counterstained with hematoxylin, dehydrated and observed for localization of calpain.

The protocol followed for calpastatin immunohistochemistry was similar to that followed for calpain. Briefly, liver sections from the non-DB (ND group) and DB mice were deparaffinised and were blocked using 3% BSA for 1 h and incubated with polyclonal anti-rabbit primary calpastatin antibody (1:300, Sigma Chemical Co., St. Louis., MO) for 14 h at 4^{o}C. A HRP conjugated secondary anti-rabbit IgG antibody (1:500) was then linked to the primary antibody before incubation with DAB, which gives a brown reaction product. The cells were counterstained with hematoxylin, dehydrated and observed for localization of calpastatin.

JPET Fast Forward. Published on October 5, 2005 as DOI: 10.1124/jpet.105.094326
This article has not been copyedited and formatted. The final version may differ from this version.

Tissue Repair

[^{3}H]-T Incorporation. S-phase DNA synthesis was measured by [^{3}H]-T incorporation into hepatonuclear DNA as described previously (Sawant et al., 2004) in the DB and non-DB mice before APAP treatment to investigate if type 2 diabetes alters S-phase DNA synthesis.

Proliferating Cell Nuclear Antigen Assay. Cell cycle progression was estimated by immunohistochemical analysis with PCNA labeled with the brown reaction product of DAB and HRP (Greenwell et al., 1991). Nuclei were counterstained lightly with hematoxylin. Observed under light microscopy, nuclei of G_0 cells were blue; cells in G_1 were stippled light brown, S-phase cell nuclei were stained dark brown, while G_2 cells had stippled light brown cytoplasmic staining with brown speckled nuclear appearance; M-cells had diffuse light brown cytoplasmic and deep blue chromosomal staining. For histomorphometric analysis, each section was observed for cells in different stages of the cell cycle in 10 high power fields (400X magnification) as reported previously (Wang et al., 2000a). One thousand cells/ slide were counted and the % number of cells in each stage was recorded.

CYP4A Western Blot Analysis. Microsomal protein (20 μg) from each mouse was separated by SDS-polyacrylamide gel electrophoresis and transferred to membranes (Wang et al., 2001). To detect CYP4A protein, nitrocellulose membranes (BioRad, Hercules, CA) were incubated with a primary goat anti-rat CYP4A polyclonal antibody (Gentest Inc., Woburn, Massachusetts). The blots were further incubated with anti-goat secondary antibody conjugated to HRP and visualized using a chemiluminescence kit obtained from Pierce Biotechnology (Bradford, IL). Immunoquantification was carried out using a GS-700

JPET Fast Forward. Published on October 5, 2005 as DOI: 10.1124/jpet.105.094326
This article has not been copyedited and formatted. The final version may differ from this version.

imaging densitometer (BioRad, Hercules, CA) followed by quantitation using Quantity One software (BioRad, Hercules, CA).

CLC Antimitotic Intervention

Treatment, Lethality, and Time Course Studies after CLC Intervention. Interventional studies with CLC were conducted to test the role of diabetes-related advancement of cells to S-phase and higher tissue repair in the type 2 DB mice. CLC is known to exert antimitosis by a combination of inhibition of DNA synthesis as indicated by decreased [^{3}H]-T incorporation by inhibition of thymidine kinase and thymidylate synthetase (Tsukamoto and Kojo, 1989) and microtubule perturbations (Manfredi and Horwitz, 1984).

On day 68 of the experimental protocol, type 2 diabetes was confirmed by measuring plasma glucose and insulin levels. On days 69 and 70, one group of DB mice (n=10/group) received CLC (2 mg/kg and 1.5 mg/kg, ip, in distilled water at 48 and 12 h before APAP administration, respectively) while the other group received distilled water (10 ml/kg, ip, vehicle control for CLC, at 48 and 12 h before APAP administration), respectively. On day 71, both the groups of DB mice received APAP (600 mg/kg, ip, in warm basic saline, pH 8). Another group of non-DB mice (ND group) treated with CLC (2 ml/kg and 1.5 ml/kg, ip, on days 69 and 70, respectively) received saline (20 ml/kg, ip) and served as controls to test any effects of CLC itself. Mice were observed thrice for the first day and then twice daily for a total of 14 days and survival and mortality were recorded.

For the time course (0 to 24 h) study, liver injury as measured by plasma ALT and AST was estimated in the non-DB (ND group only), CLC intervened DB mice (DB + CLC group), and CLC unintervened DB mice pretreated with DW (DB + DW group).

After confirming type 2 diabetes, one group of DB mice (DB + CLC group, n = 4/time point for 0 and 6 h and n = 15/time point for 12 and 24 h) were treated with two doses of

JPET Fast Forward. Published on October 5, 2005 as DOI: 10.1124/jpet.105.094326
This article has not been copyedited and formatted. The final version may differ from this version.

CLC (2 mg/kg, ip, in distilled water at 48 h) and (1.5 mg/kg, ip, in distilled water at 12 h), respectively, before APAP treatment. The other group of DB mice (DB + DW group) received distilled water (10 ml/kg, ip, n = 4/time point) and served as vehicle control. Both the DB groups (DB + CLC and DB + DW) were treated with APAP on day 71. A non-DB (ND) group [pretreated with vehicle of CLC (DW, 10 ml/kg, ip)] treated with APAP for the time course study was also maintained. The plasma and liver tissue from these mice were collected at 0, 6, 12, and 24 h after dosing with APAP (DB + CLC, DB + DW, ND + DW groups). Plasma ALT and AST were measured as biomarkers of liver injury using ThermoDMA kit # TR 7111-125 and kit # TR 7011-125, respectively.

In vivo Covalent Binding of ^{14}C-APAP-derived Radiolabel to Liver Proteins after CLC Intervention. Covalent binding of ^{14}C-APAP-derived radiolabel to liver macromolecules was estimated in the non-DB (ND group only), DB mice with and without CLC pretreatment. Livers from ND, DB mice with and without CLC intervention and treated with ^{14}C-APAP (600 mg/kg, ip, 4.3 mCi/mmol, 5 μCi/mouse, Sigma Chemical Co.) were flash frozen at 2 h after APAP treatment. Covalently bound ^{14}C-APAP-derived label to liver macromolecules was estimated using the procedure described above. Results were expressed as DPM/mg of liver protein.

Statistical Analysis

Data are expressed as means ± S.E. Comparison was made by Student's t-test. Comparison between different time points for each group and between two groups at the same time point was made by ANOVA followed by Tukey's HSD test using the factorial design and the JMP® software (SAS Institute Inc., Cary, NC). The criterion for significance was $p \leq 0.05$.

Results

Characterization of Type 2 Diabetes Mouse Model. All the DB mice survived and they appeared healthy. They exhibited weight loss but without any significant change in liver to body weight ratio, significantly higher water and food intake, and 10-fold higher urine output (70 ± 9 ml/day) compared to the non-DB mice (7 ± 1 ml/day).

On day 70, type 2 DB mice showed significant elevation in plasma glucose (128 $\pm$ 10 mg/dl in the non-DB mice (ND group) compared to 400 $\pm$ 54 mg/dl in the DB mice) and insulin levels in the normal range (1.9 $\pm$ 0.1 in non-DB (ND) mice compared to 1.7 $\pm$ 0.5 in DB mice). The ND + STZ mice exhibited normal glucose and insulin levels, however, the high fat diet fed mice exhibited 1.5 fold higher insulin levels and normal glucose levels compared to the ND group. Thus, high fat diet mice represent insulin resistant condition since these mice required 1.5 fold higher insulin to maintain normoglycemia. Figure 1 illustrates the blood glucose (panel A) and insulin (panel B) values at 0 (fasting) and 2 h after glucose challenge (5 g/kg, po). In the non-DB mice (ND group), plasma glucose values returned to normal levels at 2 h after oral glucose challenge. However, DB mice exhibited high fasting glucose (241 ± 32 mg/dl, indicated at 0 h time point in Fig. 1A) and glucose intolerance as indicated by high glucose levels at 2 h (450 ± 78 mg/dl, Fig. 1A). The insulin levels in the DB and non-DB (ND group) were similar at both 0 and 2 h after glucose administration (Fig. 1B). On the other hand, the HFD mice, inspite of normal glucose levels at 2 h after glucose treatment, exhibited insulin resistance as evidenced by higher insulin levels (~ 3-fold) at 2 h after glucose administration (Fig. 1B) compared to the ND mice. Thus, the oral glucose tolerance test proved three points: 1. Feeding high fat diet resulted in insulin resistance, 2. DB mice exhibited higher fasting glucose; and 3. Glucose intolerance was evident in DB mice.

Resistance of Type 2 Diabetic Mice to Model Hepatotoxicants.

Lethality Studies. Liver injury initiated by APAP (600 mg/kg, ip) markedly progressed in the non-DB (ND, ND + STZ, HFD) mice as indicated by 80% mortality in contrast with 80% survival of the DB mice (Table 1). Death occurred between 8 and 24 h after APAP administration. Also, bromobenzene (BB, 0.5 ml/kg, ip) and CCl_4 (1.25 ml/kg, ip) toxicity was greater in non-DB mice leading to 80 and 50% mortality in the non-DB groups compared to 80 and 70% survival of the DB mice, respectively (Table 1). The non-DB mice died between 48 and 96 h after BB or CCl_4 administration. No mortality occurred in the vehicle control DB and non-DB mice. These findings suggested that type 2 DB mice are resilient to drug and toxicant-induced hepatotoxicity. Resiliency of DB mice to APAP toxicity was chosen for further mechanistic investigation.

Hepatotoxicity. Plasma ALT (Fig. 2A) and AST (Fig. 2B) in the non-DB mice (ND, ND + STZ, HFD groups) exhibited significant increases, which correlated with the high mortality observed in this group between 8 to 24 h after APAP administration (600 mg/kg, ip).

In the non-DB groups (ND, ND + STZ, and HFD groups), 20 mice/time point/group were used at the 12, 24, 48, and 96 h time points to assure survival of 4 mice at each time point. Plasma ALT activity increased in non-DB (ND, HFD, ND + STZ groups) mice after APAP administration, peaked at 12 h and was elevated up to 24 h (Fig. 2A) resulting in 80% mortality between 8 to 24 h. The persistence and progression of liver injury over the time course are concordant with the time of mortality observed in these groups (Table 1). In the surviving non-DB mice, the injury regressed to normal by 96 h. In contrast, DB mice exhibited substantially lower liver injury at 6 (~20-fold), 12 (~24-fold), and 24 h (~6-fold) compared to non-DB (ND group) at the respective time points. In the DB mice, injury progressed up to 24 h compared to 0 h (resulting in 20% mortality between 8 to 24 h) and

then regressed to normal levels by 96 h. No significant difference in the liver injury was evident at 96 h between the surviving DB and non-DB mice. Thus, even though the DB mice showed progressive liver injury up to 24 h after APAP administration, it was significantly low compared to the non-DB mice. Plasma AST also revealed a similar pattern of liver injury (Fig. 2B) as seen with plasma ALT in both the DB and non-DB groups. In DB and non-DB groups receiving half normal saline, ALT/AST were measured at 0 (data shown), 6, 12, and 24 h after saline administration and no liver injury was evident (data not shown).

Histopathology. For comparison of histopathology, calpain, calpastatin, and PCNA results, the ND group was selected as the representative non-DB control since the extent and pattern of APAP-induced injury at respective time points in all the three non-DB (ND, HFD, ND + STZ) groups was the same. Liver sections stained with H&E were examined by light microscopy for multifocal necrosis, vacuolization, and inflammatory cell infiltration. There was no difference in the non-DB (ND group) (Fig. 3A) and DB (Fig. 3B) mice livers at 0 h. ND mice treated with APAP showed marked necrotic lesion in the liver as early as 6 h (Fig. 3C). Inflammatory cell infiltration was evident in the non-DB mice with mild to moderate coagulative necrosis at 6 h (Fig. 3C). Hepatocellular necrosis and vacuolization spread toward the periportal area with time. These effects were progressive by 12 h, manifesting severe to massive coagulative necrosis with extensive bridging of necrotic zone affecting all lobules at 12 h (Fig. 3E) compared to 0 h. From 24 h (Fig. 3G) the surviving non-DB mice showed regression of necrosis up to 48 h (data not shown) and there was no evidence of necrosis by 96 h (data not shown). On the other hand, DB mice treated with the same dose of APAP showed minimal necrosis and histological damage at 6 (Fig. 3D) and 12 h (Fig. 3F) and regression of necrosis was evident as early as 24 h (Fig. 3H).

JPET Fast Forward. Published on October 5, 2005 as DOI: 10.1124/jpet.105.094326
This article has not been copyedited and formatted. The final version may differ from this version.

APAP Bioactivation, Toxicokinetics, and Hepatic Glutathione in Diabetic Mice

For comparison of bioactivation-based mechanisms and the tissue repair response, the ND group was selected as the representative non-DB control.

1. Effect of Diabetes on Hepatic CYP2E1. Western blot analysis revealed that hepatic microsomal CYP2E1 protein in the DB mice was not different from the non-DB mice (ND and HFD groups) (Fig. 4A & B). Microsomal CYP2E1 enzyme activity (Fig. 4C) measured as *p*-nitrophenol hydroxylation was also unchanged in the DB mice relative to non-DB mice (ND group), confirming that neither hepatic microsomal CYP2E1 protein nor the enzyme activity is changed in the type 2 DB mice. However, in the HFD group (non-DB) the CYP2E1 enzyme activity was significantly lower compared to that in the ND (non-DB) group, in the absence of any change in CYP2E1 protein.

2. Covalent Binding. Total covalent binding of ^{14}C-APAP was estimated as a measure of reactive intermediate production. Covalent binding sharply increases from 30 min reaches a peak by 2 h in male SW mice (Shankar et al., 2003a). No difference was found in covalent binding ^{14}C-APAP-derived radiolabel to liver macromolecules between non-DB (ND group, 2.1 ± 0.4 DPM X 10^2/ mg protein) and DB mice (2.3 ± 0.6 DPM X 10^2/ mg protein) at 2 h after APAP administration. These data suggest that bioactivation of APAP is similar in both non-DB and DB mice.

3. APAP Toxicokinetics. Plasma APAP did not differ between the non-DB (ND group) and DB mice (Fig. 5A). Plasma $t_{1/2}$ of APAP in DB (78 ± 22 min) was the same as in non-DB (ND group, 70 ± 18 min) mice. The cumulative % of total APAP dose excreted in the urine by 12 and 24 h after APAP administration as APAP in the non-DB (ND group, 2.9 ± 0.1 and

JPET Fast Forward. Published on October 5, 2005 as DOI: 10.1124/jpet.105.094326
This article has not been copyedited and formatted. The final version may differ from this version.

5.8 ± 0.9, respectively) and DB mice (2.6 ± 0.04 and 5.7 ± 1.2, respectively) was not significantly different. Thus, plasma and urinary APAP concentrations and the plasma APAP $t_{1/2}$ were the same in the non-DB (ND group) and DB mice, indicating that altered toxicokinetics of APAP is unlikely to be the reason for protection observed in the DB mice from APAP-hepatotoxicity. However, the plasma levels of APAP-G, a nontoxic metabolite of APAP, was siginificantly lower (~32%) in the DB mice compared to non-DB (ND) mice (Fig. 5B). APAP-G represents 70 to 80% of APAP metabolism in the male SW mice (Hazelton et al., 1986; Shankar et al., 2003a). The cumulative % of total APAP dose excreted as APAP-G by the non-DB (ND) mice in urine by 12 and 24 h after APAP administration was 20.3 ± 0.3 & 78.8 ± 0.4, respectively, and in the DB mice it was 63.8 ± 2.1 & 80.8 ± 1.6, respectively. At 12 h after APAP administration, urinary elimination of APAP-G was ~31% higher in the DB mice consistent with polyurea and lower plasma levels of APAP-G in this group compared to non-DB (ND) mice. However, by 24 h the cumulative % of total APAP dose eliminated as APAP-G in both the groups was the same, indicating that there was no difference in the detoxification of APAP by glucuronidation between the two groups.

4. Hepatic Glutathione. Hepatic glutathione was unaffected by diabetes (Fig. 6). Regardless of DB condition, there was a dramatic depletion of total as well as reduced glutathione at 2 h after APAP administration. Whereas glutathione depletion was persistent in non-DB mice at 6 h after APAP treatment, that in the DB mice was largely restored back to normal by 6 h (Fig. 6). In the non-DB mice, glutathione depletion was sustained, consistent with higher liver injury observed at 6 h compared to the DB mice.

Progression /Regression of Injury

Calpain Immunohistochemistry.

JPET Fast Forward. Published on October 5, 2005 as DOI: 10.1124/jpet.105.094326
This article has not been copyedited and formatted. The final version may differ from this version.

In the present study calpain leakage was investigated in the livers of DB and non-DB mice after APAP treatment. Brown color indicated calpain-positive staining (Fig. 7). Minimal calpain staining was found in the DB and non-DB mice at 0 h (Fig. 7A & B). Notable calpain staining was primarily found in the necrotic area at 6 h (Fig. 7C) in the ND mice after APAP treatment that progressively increased resulting in intense staining at 12 h which was sustained at 24 h (Fig. 7 E and G), indicating calpain-mediated progression of liver injury. Starting at 48 h in the surviving ND mice, there was decreased calpain leakage as evidenced by decrease in calpain staining, injury regressed and complete recovery was evident at 96 h (data not shown). In contrast, the intensity and extent of calpain staining was very low over the entire time course after APAP administration in the DB mice compared to ND mice. At 6 h after APAP administration, calpain leakage was very low in the DB mice (Fig. 7D) compared to ND mice. This observation was consistent with the liver injury, which is significantly lower in the DB mice compared to the ND mice at the same time point. Moreover, during the onward time course up to 24 h, calpain leakage was substantially lower in the DB mice (Fig. 7F and H). At 48 h (data not shown) minimal calpain staining consistent with complete recovery was evident in the DB mice. These data indicate that the extent of calpain release governs the degree of progression of injury.

Tissue Repair

The objective of this study was to investigate whether in type 2 diabetes also higher number of cells advance to S-phase of cell division giving the advantages of resistance against progression of injury and early onset of tissue repair upon toxic challenge. S-phase DNA synthesis was investigated in the DB and non-DB mice by [^{3}H]-T pulse labeling and counting the number of cells in S-phase identified by PCNA immunohistochemistry (Fig. 8).

JPET Fast Forward. Published on October 5, 2005 as DOI: 10.1124/jpet.105.094326
This article has not been copyedited and formatted. The final version may differ from this version.

[^{3}H]-T Pulse Labeling Study. Stimulation of the S-phase of cell division cycle is an obligatory step in cell division and tissue repair. S-phase DNA synthesis was measured by [^{3}H]-T pulse labeling (Fig. 8A) in the non-DB (ND group) and DB livers. The [^{3}H]-T pulse labeling study revealed that DNA synthesis was increased (2-fold) in DB mice compared to the non-DB mice indicating that the S-phase DNA synthesis is significantly enhanced due to type 2 DB in SW mice.

PCNA Assay. Immunohistochemical staining of PCNA (Fig. 8) was conducted to identify and count the cells in S-phase of cell division cycle in the non-DB (ND) and DB mice livers and verify the findings of [^{3}H]-T pulse labeling study. In the non-DB (ND group) mice livers at 0 h, 95% hepatocytes were found in the G_0 phase (Fig. 8B) with only 1% of the hepatocytes in S-phase of cell cycle. After APAP treatment, minimum number of cells progressed to S-phase of cell cycle at 6 and 12 h (data not shown). Cell cycle progression was suppressed and delayed in ND mice and only in the surviving APAP treated mice was there any evidence of successful cell cycle progression. In the surviving ND mice, at 24 h significant number of cells entered S-phase progressing to G_2 and M phase by 96 h (data not shown). In contrast, in DB mice, 8-fold higher number of cells had advanced to S-phase compared to the non-DB mice confirming much higher number of S-phase cells in normally quiescent liver of these mice (Fig. 8C & D). PCNA analysis revealed 3- and 5-fold increase in the number of cells in S-phase at 12 and 24 h, respectively, after APAP administration in the DB mice compared to ND mice (data not shown). The results from PCNA analysis were consistent with the results of [^{3}H]-T pulse labeling studies confirming higher number of S-phase cells in the DB mice at 0 h compared to ND mice.

Thus, after APAP treatment, inhibited cell cycle progression in ND mice leads to progression of liver injury and mortality, while in the DB mice, diabetes-related advancement

of hepatocytes to S-phase enabled the mice to inhibit progression of injury and stimulated cell cycle progression resulted in regression of injury, restoration of liver function, and complete recovery.

Calpastatin Immunohistochemistry.

Calpastatin expression was investigated in the non-DB and DB mice with and without APAP treatment. Brown color indicated calpastatin-positive staining (Fig. 9). Minimal level of calpastatin staining was seen in the ND (non-DB) mice at 0, 6, and 12 h (Fig. 9A, C, & E) consistent with lower number of S-phase cells in the ND mice after APAP treatment. However, in the surviving ND mice, calpastatin staining was evident in the dividing/newly divided cells in the perinecrotic areas at 24 (Fig. 9G) and 96 h (data not shown). Remarkable level of calpastatin staining was found in the DB mice at 0 h (Fig. 9B) consistent with the higher number of S-phase cells in the DB mice, thereby indicating that cells in S-phase over-express calpastatin. After APAP administration (6 to 24 h), calpastatin expression was observed in larger areas of the lobule at 6 and 12 h (Fig. 9D & F), and was distributed over almost the entire lobule at 24 h (Fig. 9H) in the DB mice compared to ND mice (Fig. 9C, E & G). This observation is consistent with the greater number of cells entering and progressing in the cell division cycle in the DB mice than in the ND mice. Over-expression of calpastatin in the dividing/newly divided cells in the DB mice after APAP administration is consistent with the regression or lower progression of liver injury observed in the DB mice. These data indicate that the extent of calpastatin staining governs the calpain-mediated progression of injury.

CYP4A Expression. Resiliency of type 1 DB mice to APAP-induced hepatotoxicity is dependent on PPAR-α-mediated enhancement of liver tissue repair (Shankar et al., 2003b).

The objective of this experiment was to investigate if higher tissue repair in type 2 DB mice is mediated via PPAR-α activation. Western blot analysis revealed no difference in CYP4A expression between the non-DB and DB mice livers. These results indicate that the increased tissue repair in type 2 diabetes is not mediated via PPAR-α activation, unlike in type 1 DB mice.

Antimitotic Intervention

This experiment was conducted to examine if advancement of liver cells through cell division cycle in DB mice even before APAP administration is critical in preventing progression of liver injury initiated by bioactivation of APAP. First, lethality studies were conducted with and without CLC intervention as a test of the concept. Second, time course studies were conducted to measure liver injury as assessed by plasma transaminases. Third, covalent binding of ^{14}C-APAP-derived radiolabel to liver tissue was examined as a measure of APAP bioactivation with and without CLC intervention.

Lethality Study After CLC Intervention. DB mice pretreated with CLC 48 (2 mg/kg, ip) and 12 h (1.5 mg/kg, ip) before APAP administration exhibited inhibition of 8-fold increase in the number of S-phase cells in type 2 DB mice as estimated by PCNA immunohistochemistry (data not shown). APAP-induced mortality was 70% in the CLC intervened DB mice (Table 2). Eighty % of the DB mice not intervened with CLC but receiving the same dose of APAP (600 mg/kg, ip) survived suggesting a pivotal role of diabetes-related advancement of cells to S-phase in the DB-induced resistance (Table 2). Deaths in ND mice and CLC intervened DB mice receiving APAP occurred during the same time frame (8 to 24 h, Tables 1 & 2) suggesting that protective mechanism of DB was abolished by CLC intervention. DB + DW and ND mice treated with CLC + saline alone did

JPET Fast Forward. Published on October 5, 2005 as DOI: 10.1124/jpet.105.094326
This article has not been copyedited and formatted. The final version may differ from this version.

not show any signs of toxicity. These results underscore the critical importance of cell division and tissue repair in imparting a survival advantage to the DB mice challenged with a lethal dose of APAP.

Hepatotoxicity After CLC Intervention. If liver cells advancing to S-phase or other phases of cell division is critical for hepatoprotection by preventing the progression of injury, CLC intervention before APAP exposure should lead to two effects in the DB mice. First, initial injury of APAP should not change. Second, initiated liver injury should expand by progression because the resistance, which would have come with cells advancing in cell division cycle, is lacking. To examine these effects, a time course (0 to 24 h) study was conducted. Plasma ALT and AST (Fig. 10A & B) elevations in the CLC intervened DB mice (DB + CLC group) at 2 h after APAP administration was not different from unintervened DB mice (DB + DW) and the same as observed earlier (Fig. 2) indicating that initiation of APAP injury was not affected. However, by 6 h liver injury was expanding in the CLC intervened DB mice and progression of injury continued, culminating in 70% mortality. The CLC intervened DB mice exhibited substantially high liver injury at 6 (~18-fold), 12 (~22-fold), and 24 h (~6-fold) compared to the unintervened DB mice (DB + DW). These increases in the CLC intervened DB mice are comparable to transaminase elevations in ND group compared to the DB mice receiving the same dose of APAP.

In the DB + CLC group, 15 mice/time point/group were used at the 12 and 24 h time points to assure survival of 4 mice at each time point. In the ND group, plasma ALT activity increased after APAP administration peaked at 12 h and was elevated till 24 h (Fig. 10A) as observed earlier (Fig. 2) resulting in 80% mortality between 8 to 24 h. The liver injury in the DB + CLC mice was not significantly different from the ND group at 6 and 12 h except for 24 h where the liver injury was ~ 2-fold lower in the CLC intervened DB mice compared to

ND mice after APAP administration. Plasma AST also revealed a similar pattern of liver injury (Fig. 10B) as seen with plasma ALT in the DB + DW, DB + CLC and ND groups. These results indicate that expansion of initiated injury destroys the liver in ND and CLC intervened DB mice receiving APAP. Conversely, it is lack of expansion or progression of injury initiated by APAP that protects the DB mice.

Covalent Binding After CLC Intervention. No difference was found in covalent binding of ^{14}C-APAP-derived radiolabel to liver macromolecules between non-DB (ND, 2.1 ± 0.4 DPM X 10^2/ mg protein), CLC unintervened DB mice (DB + DW, 2.3 ± 0.6 DPM X 10^2/ mg protein) and CLC intervened DB mice (DB + CLC, 2 ± 0.3 DPM X 10^2/ mg protein) at 2 h after APAP administration. These data suggest that CLC intervention did not alter the covalent binding of ^{14}C-APAP-derived radiolabel to liver macromolecules compared to the unintervened DB mice (DB + DW).

Discussion

DB patients have nearly two-fold higher risk of acute liver failure, chronic liver failure, and hepatocarcinogenesis (El-Serag and Everhart, 2002; El-Serag et al., 2004). Several studies in DB rats indicate that both type 1 and type 2 diabetes are predisposing factors for hepatic sensitivity to drugs and toxicants (El-Hawari and Plaa, 1983; Grant and Duthie, 1988; Watkins et al., 1988; Wang et al., 2000a; Sawant et al., 2004). However, marked species difference in hepatotoxic sensitivity exists between type 1 DB rats and mice (Shankar et al., 2003a; Wang et al., 2000a). Type 1 DB rats are sensitive to TA-induced hepatotoxicty due to compromised liver tissue repair (Wang et al., 2000a). In contrast, type 1 DB mice are resistant to several hepatotoxicants. Studies after APAP treatment (600 mg/kg, ip) revealed that protection in the type 1 DB mice is predominantly due increased PPAR-α-dependent compensatory tissue repair which prevents APAP-initiated liver injury from progressing (Shankar et al., 2003a; Shankar et al., 2003b).

Surprisingly, very few studies have investigated the effect of type 2 diabetes on sensitivity of hepatotoxicants, even though it is the most prevalent form of diabetes, representing 90-95% of the DB population. Sawant et al. (2004) reported for the first time that the type 2 DB rats are sensitive to hepatotoxicity of several model hepatotoxicants including CCl_4. Mechanistic studies revealed that the increased sensitivity to CCl_4 and TA hepatotoxicity is due to inhibited compensatory tissue repair (Sawant et al., 2004; Sawant et al., 2005). In the present work, to investigate whether or not species difference exists for hepatotoxic sensitivity of type 2 DB, sensitivity of type 2 DB mice was studied using CCl_4, BB, and APAP. For this purpose the protocol used to induce diabetes in rats (Sawant et al., 2004) was adapted with modification to induce diabetes in mice. The type 2 DB mouse model based on feeding high fat diet for 2 months followed by a single dose of STZ exhibits hyperglycemia, normoinsulinemia, and oral glucose intolerance on day 10 after STZ administration (Fig. 1).

In stark contrast to our findings in type 2 DB rats, lethality studies revealed that type 2 DB mice are protected from hepatotoxicity and mortality induced by model hepatotoxicants such as CCl_4, BB, and APAP, indicating a marked species difference in the sensitivity of type 2 diabetes to drug- and toxicant-induced hepatotoxicity. Using APAP as a model hepatotoxicant, mechanisms of protection in type 2 DB mice were investigated. Time course studies of liver injury revealed that even though liver injury was same at 2 h, progression of liver injury was dramatically lower in the DB mice compared to the non-DB mice. While this may be explained by several potential mechanisms, for this study the following four leading mechanisms were investigated: (1) decreased bioactivation of APAP; (2) increased detoxification via glucuronide and glutathione conjugation of APAP; (3) advancement of hepatocytes in cell division cycle in the type 2 DB mice favorably influencing liver tissue repair after APAP administration; and (4) progression of APAP-initiated liver injury is prevented because calpain is inhibited by over-expression of calpastatin in dividing/newly divided cells.

First and foremost, decreased bioactivation of APAP due to lower hepatomicrosomal CYP2E1 expression and activity and lower ^{14}C-APAP covalent binding were investigated. In the type 2 DB mice, CYP2E1 protein, its enzyme activity (Fig. 4B & 4C) and covalent binding of ^{14}C-APAP-derived radiolabel to liver macromolecules was not different compared to non-DB mice, indicating that the initial bioactivation-based liver injury is the same in DB and non-DB mice. Our present findings in the DB mice are consistent with the unaltered CYP2E1 in type 2 DB rats. In the high fat diet based type 2 DB rats neither the CYP2E1 protein nor activity was altered (Sawant et al., 2004) compared to non-DB rats. Our previous findings in type 2 DB rats and present findings in the mice are consistent with the unchanged CYP2E1 protein and mRNA in type 2 DB ob/ob mice and Zucker rats (Novak and Woodcraft, 2000). Thus, in these rodent models of type 2 diabetes, the emerging picture

indicates that liver microsomal CYP2E1 does not change significantly. In contrast, in type 1 DB, a different and divergent picture is emerging. In STZ-induced type 1 DB rats, liver microsomal CYP2E1 protein and enzyme activity are markedly increased (Wang et al., 2000b), while in type 1 DB mice a small, but significant (30%) decrease occurs (Shankar et al., 2003a). Sakuma et al. (2001) have also reported a similar species difference in the modulation of hepatic CYP2E1 between STZ-induced type 1 DB rats and mice. In type 2 DB patients, contradictory evidence of increased CYP2E1 (Wang et al., 2003) and unchanged CYP2E1 protein and activity (Lucas et al., 1998) has been reported.

The second potential mechanism is increased glucuronidation and glutathione conjugation of APAP in the type 2 DB mice. Diabetes is associated with increased water intake, altered kidney architecture and kidney function (Shankar et al., 2003a), and consequently 10-fold higher urine output. Thus, it is reasonable to expect that type 2 diabetes may alter toxicokinetics of APAP. However, our studies revealed no difference between non-DB (ND) and DB mice in plasma APAP levels, plasma APAP t½ and the urinary excretion of APAP. In the SW mice employed in the current study APAP-G conjugate represents 70 to 80%, while APAP-sulfate represents 5 to 7% of APAP metabolism (Hazelton et al., 1986; Shankar et al., 2003a). Therefore, a significant change in the detoxification of APAP by glucuronidation in the type 2 DB mice may be expected to impact initiation of APAP-induced liver injury. Plasma APAP-G levels were 32% lower consistent with 31% increased urinary excretion of APAP-G in the type 2 DB mice compared to ND mice at 12 h after APAP treatment. However, by 24 h the cumulative % of APAP dose excreted as APAP-G was same in both the groups, obviating increased detoxification of APAP by glucuronidation as a mechanism of protection in DB mice. It is clear that the lower plasma levels of APAP-G in DB mice is a reflection of more rapid excretion of this metabolite in urine as a result of polyurea associated with diabetes.

Higher liver glutathione (GSH) content is a very important indicator of whether detoxification of reactive metabolite of APAP is higher in DB mice, and whether it affords greater hepatoprotection as an antioxidant in the DB mice. Glutathione levels at the initial time points when the injury begins are critical for the hepatoprotective action while at later time points when the injury has progressed drastically, glutathione levels may be affected because of the extent of injury. The present study indicated that type 2 diabetes does not change GSH status of the liver (Fig. 6). Depletion of hepatic glutathione was same in the DB and non-DB mice at 2 h after APAP administration, while higher glutathione levels in the DB mice at 6 h compared to non-DB mice may be a consequence of 20-fold lower injury in the DB mice compared to non-DB mice, indicating that increased glutathione conjugation may not be the underlying mechanism of protection observed in the DB mice from APAP hepatotoxicity. Thus, no change in hepatic CYP2E1 protein and enzyme activity, lack of difference in covalent binding of ^{14}C-APAP-derived radiolabel to liver macromolecules and lack of significant difference in hepatic glutathione levels between the DB and non-DB mice collectively suggest that decreased bioactivation and increased detoxification are unlikely to explain diabetes-induced protection from APAP-hepatotoxicity.

The third potential mechanism for protection from progression of APAP-initiated liver injury in the type 2 DB mice is advancement of hepatocytes in cell division cycle that may confer resistance against progression of APAP-initiated injury, and favor a higher tissue repair response after APAP administration. The present study revealed that type 2 DB mice have 8-fold higher number of cells in S-phase of the cell division cycle compared to non-DB mice, indicating that advancement of cells in cell division cycle in the DB mice results in protection from progression of APAP-initiated liver injury. To address the question of whether increased advancement of hepatocytes in cell division cycle in type 2 DB mice is indeed the critical event, CLC antimitotic intervention study was conducted. CLC

intervention 48 and 12 h before APAP treatment abolished the protection due to diabetes resulting in 70% mortality in the CLC intervened DB mice (DB + CLC) receiving APAP compared to 20% mortality in the CLC unintervened DB mice (DB + DW) receiving the same dose of APAP. CLC intervention inhibited the diabetes-associated advancement of cells in the cell division cycle and the initial liver injury of APAP was same in CLC intervened (DB + CLC) and unintervened DB (DB + DW) mice. However, APAP-initiated liver injury progressed culminating in liver failure and death only in the CLC intervened DB mice challenged with APAP. To rule out the possibility that CLC intervention may have affected APAP-bioactivation, covalent binding of ^{14}C-APAP-derived radiolabel to liver tissue was measured. Lack of any difference in covalent binding of ^{14}C-APAP-derived radiolabel to liver macromolecules and the identical initial liver injury in the DB + CLC and DB + DW groups of mice, indicates that CLC-pretreatment does not alter the initial bioactivation-based injury. Thus, inhibition of higher number of S-phase cells or tissue repair in the CLC intervened DB mice results in progression of APAP-initiated liver injury. Our results are consistent with several studies that have reported the importance of robust compensatory tissue repair response in determining the final outcome of toxicity (Mangipudy et al., 1995; Ramaiah et al., 1998; Soni et al., 1999; Wang et al., 2001; Mehendale 2005). Furthermore, inhibition of cell division via antimitotic intervention with CLC has been shown to result in progression of injury from nonlethal doses of TA (Mangipudy et al., 1996), CCl_4 (Rao and Mehendale, 1991; Rao and Mehendale, 1993), and APAP (Shankar et al., 2003a). Thus, the markedly lower progression of APAP-initiated liver injury in type 2 DB mice is due to increased advancement of cells in the cell division cycle.

Another important finding from our study is lower calpain leakage and lower progression of APAP-initiated injury in the DB mice compared to greater calpain-mediated progression of injury in the non-DB mice. Limaye et al. (2003) have shown that leakage of calpain, a

hydrolytic enzyme, from the dying hepatocytes causes progression of injury following APAP-induced necrosis in mice and after CCl_4-induced necrosis in rats. Calpain inhibition either by over-expression of calpastatin (Limaye et al., 2005; Mehendale and Limaye, 2005), an endogenous inhibitor of calpain, in dividing/newly divided cells or by administration of a synthetic inhibitor of calpain results in regression of APAP-initiated injury (Limaye et al., 2003). Therefore, the fourth potential mechanism we investigated is whether increasing leakage of calpain in the intercellular space in the livers of APAP treated ND mice is in concordance with the progression of APAP-initiated injury and whether calpastatin over-expression is commensurate with the remarkably inhibited injury in the DB mice after APAP administration. First, in the APAP treated ND mice there was evidence of progressively increasing leakage of calpain in the intercellular space concordant with the progression of liver injury and death in mice. Only in the surviving 20% of the mice did the appearance of intercellular calpain decline. In the DB mice receiving APAP, while initially calpain did appear in the intercellular space, the over-expression of calpastatin incapacitated the degradative action of intercellular calpain. Calpastatin was over-expressed in DB mice owing to the advancement of hepatocytes to S-phase. In contrast, in the ND mice, lack of such advancement of hepatocytes to S-phase and hence lack of calpastatin expression allowed APAP-initiated liver injury to progress through calpain-mediation. Therefore, these findings are consistent with inhibited progression of APAP-initiated injury by over-expressed calpastatin in the DB mice.

Why do cells advance in cell division cycle in the DB mice? In the type 1 DB mice, resiliency of type 1 DB mice to APAP-initiated liver injury is dependent on PPAR-α-mediated higher liver repair (Shankar et al., 2003b). Therefore, whether or not PPAR-α is activated in livers of type 2 DB mice was investigated in the present study. CYP4A expression, a marker of PPAR-α activation, was not different in type 2 DB mice compared to

non-DB (ND) mice suggesting that the higher tissue repair in type 2 DB mice is independent of PPAR-α activation. Studies to understand mechanisms of higher advancement of cells in cell division cycle in the DB mice are worthy of further investigations.

In conclusion, four significant aspects of the present study are: first, in addition to the previously established resistance of type 1 DB mice to hepatotoxicants, the findings of this study indicate that type 2 DB mice are also resistant to hepatotoxic drugs and toxicants; second, a significant number of normally quiescent hepatocytes of the adult mice, advance to S-phase of cell division in type 2 diabetes making these cells resistant to the destructive action of calpain on one hand and favoring promptly stimulated robust compensatory liver tissue repair upon exposure to APAP on the other; third, over-expression of calpastatin in dividing/newly divided cells inhibits the destructive actions of calpain preventing the progression of APAP-initiated liver injury; fourth, marked species difference in hepatotoxic sensitivity between DB mice and DB rats and similarity of DB rats and DB patients to hepatotoxic sensitivity suggests that the type 2 DB rat model may be representative of DB patients and could be used for testing hepatotoxic sensitivity.

Acknowledgements

Sharmilee P. Sawant is a recipient of predoctoral fellowship award from American Heart Association, Southern Affiliate, and their support is gratefully acknowledged.

References

Bailey CJ and Flatt PR (1991) Animal models of non-insulin dependent diabetes mellitus, in *Textbook of Diabetes*. (Pickup J. Williams G eds): pp 228-239 Blackwell Scientific, London UK.

Chen C, Hennig GE, and Manautou JE (2003) Hepatobiliary excretion of acetaminophen glutathione conjugate and its derivatives in transport-deficient (TR-) hyperbilirubinemic rats. *Drug Metab Dispos* **31**: 798-804.

Chipman JK, Kurukgy M, and Walker CH (1979) Comparative metabolism of a dieldrin analogue: hepatic microsomal systems as models for metabolism in the whole animal. *Biochem Pharmacol* **28**: 69-75.

Corcoran GB, Racz WJ, Smith CV, and Mitchell JR (1985) Effects of N-acetylcysteine on acetaminophen covalent binding and hepatic necrosis in mice. *J Pharmacol Exp Ther* **232**: 864-872.

Dargan PI and Jones AL (2003) Management of paracetamol poisoning. *Trends Pharmacol Sci* **24**: 154-157.

Dnyanmote AV, Sawant SP, Edward LA, Latendresse JR, Warbritton AA, and Mehendale HM (2005) Diabetic mice are protected from normally lethal nephrotoxicity of S-1, 2 dichlorovinyl–*L*-cysteine (DCVC): role of nephrogenic tissue repair. *Toxicol Appl Pharmacol* 210: 000-000.

El-Hawari AM and Plaa GL (1983) Potentiation of thioacetamide-induced hepatotoxicity in alloxan- and streptozotocin-diabetic rats. *Toxicol Lett* **17**: 293-300.

El-Serag HB and Everhart JE (2002) Diabetes increases the risk of acute hepatic failure. *Gastroenterology* **122**: 1822-1828.

El-Serag HB, Tran T, and Everhart JE (2004) Diabetes increases the risk of chronic liver disease and hepatocellular carcinoma. *Gastroenterology* **126**: 460-468.

Grant MH and Duthie SJ (1988) The cytotoxicity of menadione in hepatocytes isolated from streptozotocin-induced diabetic rats. *Biochem Pharmacol* **37**: 3793-3796.

Greenwell A, Foley JF, and Maronpot RR (1991) An enhancement method for immunohistochemical staining of proliferating cell nuclear antigen in archival rodent tissues. *Cancer Lett* **59**: 251-256.

Hazelton GA, Hjelle JJ, and Klaassen CD (1986) Effects of butylated hydroxyanisole on acetaminophen hepatotoxicity and glucuronidation in vivo. *Toxicol Appl Pharmacol* **83**:474-485.

Jaeschke H (1990) Glutathione disulfide formation and oxidant stress during acetaminophen-induced hepatotoxicity in mice in vivo: the protective effect of allopurinol. *J Pharmacol Exp Ther* **255**: 935-941.

Limaye PB, Apte UM, Shankar K, Bucci TJ, Warbritton A, and Mehendale HM (2003) Calpain released from dying hepatocytes mediates progression of acute liver injury induced by model hepatotoxicants. *Toxicol Appl Pharmacol* **191**: 211-226.

Limaye PB, Bhave VS, Palkar PS, Apte UM, Latendresse JR, Yu S, Kashireddy P, Reddy JK, and Mehendale HM (2005) Calpastatin over-expression protects against toxicant-induced progression of injury associated with acute liver failure in mice. *The Toxicologist* **84**: 77.

Lucas D, Farez C, Bardou LG, Vaisse J, Attali JR, and Valensi P (1998) Cytochrome P450 2E1 activity in diabetic and obese patients as assessed by chlorzoxazone hydroxylation. *Fundam Clin Pharmacol* **12**: 553-558.

Manfredi JJ and Horwitz SB (1984) Vinblastine paracrystals from cultured cells are calcium-stable. *Exp Cell Res* **150**: 205-212.

Mangipudy RS, Chanda S, and Mehendale HM (1995) Tissue repair response as a function of dose in thioacetamide hepatotoxicity. *Environ Health Perspect* **103**: 260-267.

Mangipudy RS, Rao PS, and Mehendale HM (1996) Effect of an antimitotic agent colchicine on thioacetamide hepatotoxicity. *Environ Health Perspect* **104**: 744-749.

Mehendale HM and Limaye PB (2005) Calpain: a death protein that mediates progression of liver injury. *Trends Pharmacol Sci* **26**: 232-236.

Mehendale HM (2005) Tissue repair: an important determinant of final outcome of toxicant-induced injury. *Toxicol Pathol* **33**: 41-51.

Mitchell JR, Jollow DJ, Potter WZ, Davis DC, Gillette JR, and Brodie BB (1973) Acetaminophen-induced hepatic necrosis. I. Role of drug metabolism. *J Pharmacol Exp Ther* **187**: 185-194.

Novak RF and Woodcroft KJ (2000) The alcohol-inducible form of cytochrome P450 (CYP 2E1): role in toxicology and regulation of expression. *Arch Pharm Res (NY)* **23:** 267-282.

Portha B, Serradas P, Bailbe D, Suzuki K, Goto Y and Giroix MH (1991) Beta-cell insensitivity to glucose in the GK rat, a spontaneous nonobese model for type 2 diabetes. *Diabetes* **40:**486-491.

Ramaiah SK, Bucci TJ, Warbritton A, Soni MG, and Mehendale HM (1998) Temporal changes in tissue repair permit survival of diet-restricted rats from an acute lethal dose of thioacetamide. *Toxicol Sci* **45**: 233-241.

Rao VC and Mehendale HM (1993) Effect of antimitotic agent colchicine on carbon tetrachloride toxicity. *Arch Toxicol* **67**: 392-400.

Sakuma T, Honma R, Maguchi S, Tamaki H, and Nemoto N (2001) Different expression of hepatic and renal cytochrome P450s between the streptozotocin-induced diabetic mouse and rat. *Xenobiotica* **31**: 223–237.

Sawant SP, Dnyanmote AV, Shankar K, Limaye PB, Latendresse JR, and Mehendale HM (2004) Potentiation of carbon tetrachloride hepatotoxicity and lethality in type 2 diabetic rats. *J Pharmacol Exp Ther* **308**: 694-704.

Sawant SP, Dnyanmote AV, Warbritton A, Latendresse JR, and Mehendale HM (2005) Type 2 diabetic rats are sensitive to thioacetamide hepatotoxicity. *Toxicol Appl Pharmacol* **211:** 000-000.

Shankar K, Vaidya VS, Apte UM, Manautou JE, Ronis MJ, Bucci TJ, and Mehendale HM (2003a) Type 1 diabetic mice are protected from acetaminophen hepatotoxicity. *Toxicol Sci* **73**: 220-234.

Shankar K, Vaidya VS, Corton JC, Bucci TJ, Liu J, Waalkes MP, and Mehendale HM (2003b) Activation of PPAR-alpha in streptozotocin-induced diabetes is essential for resistance against acetaminophen toxicity. *Faseb J* **17**: 1748-1750.

Shankar K, Vaidya VS, Wang T, Bucci TJ, and Mehendale HM (2003c) Streptozotocin-induced diabetic mice are resistant to lethal effects of thioacetamide hepatotoxicity. *Toxicol Appl Pharmacol* **188**: 122-134.

Soni MG, Ramaiah SK, Mumtaz MM, Clewell H, and Mehendale HM (1999) Toxicant-inflicted injury and stimulated tissue repair are opposing toxicodynamic forces in predictive toxicology. *Regul Toxicol Pharmacol* **29**:165-174.

Tsukamoto I and Kojo S (1989) Effect of colchicine and vincristine on DNA synthesis in regenerating rat liver. *Biochim Biophys Acta* **1009**: 191-193.

Wang T, Fontenot RD, Soni MG, Bucci TJ, and Mehendale HM (2000a) Enhanced hepatotoxicity and toxic outcome of thioacetamide in streptozotocin-induced diabetic rats. *Toxicol Appl Pharmacol* **166**: 92-100.

Wang T, Shankar K, Bucci TJ, Warbritton A, and Mehendale HM (2001) Diallyl sulfide inhibition of CYP2E1 does not rescue diabetic rats from thioacetamide-induced mortality. *Toxicol Appl Pharmacol* **173**:27-37.

Wang T, Shankar K, Ronis MJ, and Mehendale HM (2000b) Potentiation of thioacetamide liver injury in diabetic rats is due to induced CYP2E1. *J Pharmacol Exp Ther* **294**: 473-479.

Wang Z, Hall SD, Maya JF, Li L, Asghar A, and Gorski JC (2003) Diabetes mellitus increases the in vivo activity of cytochrome P450 2E1 in humans. *Br J Clin Pharmacol* **55**: 77-85.

Watkins JB, 3rd, Sanders RA, and Beck LV (1988) The effect of long-term streptozotocin-induced diabetes on the hepatotoxicity of bromobenzene and carbon tetrachloride and hepatic biotransformation in rats. *Toxicol Appl Pharmacol* **93**: 329-338.

Zaher H, Buters JT, Ward JM, Bruno MK, Lucas AM, Stern ST, Cohen SD, and Gonzalez FJ (1998) Protection against acetaminophen toxicity in CYP1A2 and CYP2E1 double-null mice. *Toxicol Appl Pharmacol* **152**: 193-199.

JPET Fast Forward. Published on October 5, 2005 as DOI: 10.1124/jpet.105.094326
This article has not been copyedited and formatted. The final version may differ from this version.

Footnotes

[a] Send reprint requests to:

Dr. Harihara M. Mehendale

Department of Toxicology

College of Pharmacy

The University of Louisiana -Monroe

700 University Avenue

Monroe, LA 71209-0470

USA

E-mail: mehendale@ulm.edu

Financial support:

This study was supported by The Louisiana Board of Reagents Fund through The University of Louisiana at Monroe, Kitty DeGree Chair in Pharmacy (Toxicology).

Legends for Figures

Fig. 1. Effect of type 2 diabetes on glucose and insulin in oral glucose intolerance test in male SW mice. Male SW mice were fed either normal diet or high fat diet for 2 months and on day 60 were injected either STZ (120 mg/kg, ip, in 0.01 M citrate buffer, pH 4.3) or citrate buffer (10 ml/kg, ip). Injecting STZ to high fat diet fed mice (HFD + STZ) induced type 2 diabetes. On day 70, plasma glucose and insulin levels were estimated as mentioned in Materials and methods section. On day 71, DB and non-DB mice were administered glucose solution (20 % glucose solution, 5 g/kg, po). Blood samples were collected under diethyl ether anesthesia at 0 and 2 h after glucose administration. Plasma glucose and insulin levels from these samples were estimated as described under the Materials and methods section. *Significantly different from respective 0 h time point; [!]Significantly different from the non-DB normal diet fed control injected citrate buffer (ND group) at the same time point. $p \leq 0.05$.

Fig. 2. Effect of type 2 diabetes on liver injury by APAP treatment in male SW mice. Panel A. Plasma alanine aminotransferase (ALT) and Panel B. aspartate aminotransferase (AST) activities over a time course after APAP administration. Mice were made DB as described in Fig. 1. On day 71, DB and non-DB mice received APAP (600 mg/kg, ip, in warm basic saline, pH 8). Blood samples were collected under diethyl ether anesthesia at various time points (0-96 h) after APAP administration (n = 4/time point/group except for non-DB groups n =20 at 12, 24, 48, and 96 h time points to allow survival of enough mice for time course studies). *Significantly different from respective 0 h time point; [!]Significantly different from the non-DB normal diet fed control injected citrate buffer (ND group) at the same time point. $p \leq 0.05$.

JPET Fast Forward. Published on October 5, 2005 as DOI: 10.1124/jpet.105.094326
This article has not been copyedited and formatted. The final version may differ from this version.

Fig. 3. Effect of type 2 diabetes on APAP-induced hepatic necrosis in male SW mice. Typical photomicrographs of liver sections from non-DB mice (ND group) (right) and DB mice (HFD + STZ group) (left) at 0, 6, 12, and 24 h after APAP administration. Panel A, C, E, & G: non-DB (ND group) mice 0, 6, 12, & 24 h post treatment with APAP. Panel B, D, F, & H: DB mice 0, 6, 12, & 24 h post-treatment with APAP. c, central vien; N, areas of necrosis. H&E original magnification 200X.

Fig. 4. Effect of type 2 diabetes on hepatomicrosomal CYP2E1 expression and enzyme activity in male SW mice. Mice were made DB as mentioned in Fig. 1. On day 71, liver samples were collected under diethyl ether anesthesia and microsomes were prepared ($n = 3$). A representative CYP2E1 blot is shown in the upper panel, A; panel B, microsomal CYP2E1 protein was detected by Western blot and quantified by densitometry; CYP2E1 activity was measured by PNP–hydroxylase assay (panel C). [!]Significantly different from the non-DB normal diet fed control injected citrate buffer (ND group) at the same time point. $p \leq 0.05$.

Fig. 5. Effect of type 2 diabetes on plasma levels of APAP and APAP-glucuronide (APAP-G) in male SW mice. Plasma samples were collected as mentioned in Materials and methods section. Plasma APAP levels were measured over a time course (0-720 min) after APAP administration (600 mg/kg, ip, n = 3 per time point per group) (Panel A) and plasma APAP-glucuronide (APAP-G) levels were measured over a time course (0-720 min) after APAP administration (600 mg/kg, ip). [!]Significantly different from the non-DB normal diet fed control injected citrate buffer (ND group) at the same time point. $p \leq 0.05$.

Fig. 6. Hepatic glutathione levels after APAP treatment. Panel A: Diabetes was induced as described in Materials and methods. Hepatic glutathione levels (total and reduced) were

JPET Fast Forward. Published on October 5, 2005 as DOI: 10.1124/jpet.105.094326
This article has not been copyedited and formatted. The final version may differ from this version.

estimated at 0, 2, and 6 h after APAP treatment (600 mg/kg, ip, n = 4/time point/group) in non-DB (ND group) and DB mice. See Materials and methods for details. *Significantly different from respective 0 h time point; [!]Significantly different from the non-DB normal diet fed control injected citrate buffer (ND group) at the same time point. $p \leq 0.05$.

Fig. 7. Effect of type 2 diabetes on calpain leakage after APAP-induced liver injury in male SW mice. Typical photomicrographs of liver sections from non-DB mice (ND group) (right) and DB mice (HFD + STZ group) (left) at 0, 6, 12, and 24 h after APAP administration. Panel A, C, E, & G: non-DB (ND group) mice 0, 6, 12, and 24 h post treatment with APAP. Panel B, D, F, & H: DB mice 0, 6, 12, and 24 h post-treatment with APAP. c, central vien; Brown color indicates calpain-positive staining shown by arrows. Original magnification 100X.

Fig. 8. Effect of type 2 diabetes on liver tissue repair in male SW mice. [^{3}H]-T incorporation into hepatonuclear DNA in non-DB (ND group) and DB mice (A); PCNA immunohistochemistry between liver sections of non-DB (ND group) and DB mice (B, C, and D). Typical photomicrographs of liver sections from non-DB mice (ND group) and DB mice (HFD + STZ group) (left). Hepatocytes in S-phase are with dark-brown nuclear staining. Panel B: non-DB mouse liver (ND group) and Panel C: DB mouse liver.. Original magnification 400X; histomorphometric analysis of cells in S-phase in livers from non-DB mice (ND group) and DB mice (Panel D). Treatment details are as in Fig. 1. [!]Significantly different from the non-DB normal diet fed control injected citrate buffer (ND group) at the same time point. $p \leq 0.05$.

JPET Fast Forward. Published on October 5, 2005 as DOI: 10.1124/jpet.105.094326
This article has not been copyedited and formatted. The final version may differ from this version.

Fig. 9. Effect of type 2 diabetes on calpastatin expression after APAP treatment in male SW mice. Typical photomicrographs of liver sections from non-DB mice (ND group) (right) and DB mice (HFD + STZ group) (left) at 0, 6, 12, and 24 h after APAP administration. Panel A, C, E, & G: non-DB (ND group) mice 0, 6, 12, & 24 h post treatment with APAP. Panel B, D, F, & H: DB mice 0, 6, 12, & 24 h post-treatment with APAP. c, central vien. Brown color indicates calpastatin-positive staining shown by arrows. Original magnification 200X.

Fig. 10. Effect of type 2 diabetes on liver injury by APAP treatment in male SW mice after CLC intervention. Panel A. Plasma alanine aminotransferase (ALT) and Panel B. aspartate aminotransferase (AST) activities over a time course after APAP administration. Mice were made DB as described in Fig. 1. After confirming type 2 diabetes on day 68, on days 69 and 70, one group of DB mice (DB + CLC group, n = 4/time point for 0 and 6 h and n = 15/time point for 12 and 24 h) were treated with two doses of CLC (2 mg/kg, ip, in distilled water at 48 h) and (1.5 mg/kg, ip, in distilled water at 12 h), respectively, before APAP treatment. The other group of DB mice (DB + DW group) received distilled water (10 ml/kg, ip, n = 4/time point) and served as vehicle control. Both the DB groups (DB + CLC and DB + DW) were treated with APAP on day 71. The non-DB (ND) group [pretreated with vehicle of CLC (DW, 10 ml/kg, ip)] was treated with APAP for the time course study. Blood samples were collected under diethyl ether anesthesia at various time points (0-24 h) after APAP administration (n = 4/time point/group except for ND and DB + CLC groups n = 15 at 12 and 24 h time points to allow survival of enough mice for time course studies). *Significantly different from respective 0 h time point; [!]Significantly different from the non-DB normal diet fed control injected citrate buffer (ND group) at the same time point, [#]Significantly different from the CLC unintervened DB mice (DB + DW) at the same time point. $p \leq 0.05$.

JPET Fast Forward. Published on October 5, 2005 as DOI: 10.1124/jpet.105.094326
This article has not been copyedited and formatted. The final version may differ from this version.

TABLE 1

Effect of Type 2 Diabetes on Toxicity of Acetaminophen (APAP), Bromobenzene (BB), and CCl_4 in Male Swiss Webster Mice[a]

Treatment	Non-diabetic (Non-DB)			Diabetic (DB)
	Normal diet fed mice		High Fat Diet fed mice	
	ND	ND + STZ	HFD	HFD + STZ
% Mortality, N = 10/group				
APAP (600 mg/kg, ip)	80 [b]	80 [b]	80 [b]	20 [b]
BB (0.5 ml/kg, ip)	80 [c]	80 [c]	80 [c]	20 [c]
CCl_4 (1.25 ml/kg, ip)	50 [c]	50 [c]	50 [c]	30 [c]

[a] Male SW Mice were fed either high fat diet or normal diet. On day 60, male SW mice were injected with either STZ (120 mg/kg, ip, in citrate buffer, pH 4.3) or citrate buffer (10 ml/kg, ip) alone. On day 71, all DB [high fat diet mice treated with streptozotocin (STZ)] and non-DB groups [normal diet fed mice treated with either STZ (ND + STZ) or vehicle (ND), high fat diet fed mice injected vehicle (HFD)] were injected with single dose of acetaminophen (APAP, 600 mg/kg, ip, in warm basic saline, pH 8), carbon tetrachloride (CCl_4, 1.25 ml/kg, ip, in corn oil) or bromobenzene (BB, 0.5 ml/kg, ip, in corn oil). Survival and mortality were observed thrice on the first day and twice daily thereafter for a total of 14 days. No mortality was observed in the vehicle treated DB and non-DB mice. Number of deaths and time were recorded.

[b] All deaths occurred between 8 and 24 h after toxicant challenge.

[c] All deaths occurred between 48 and 72 h after toxicant challenge.

JPET Fast Forward. Published on October 5, 2005 as DOI: 10.1124/jpet.105.094326
This article has not been copyedited and formatted. The final version may differ from this version.

TABLE 2

Effect of Colchicine Antimitotic Intervention on Acetaminophen (APAP)-induced Mortality in Type 2 Diabetic Mice[a]

Treatment Groups	Dose of APAP (mg/kg)	Total No. of mice	Mortality No. of mice	% Survival
DB mice + DW + APAP	600	10	2[b]	80
DB mice + CLC + APAP	600	10	7[b]	30
DB mice + CLC + saline	-	10	0	0
Non-DB (ND group) mice + CLC + saline	-	10	0	0

[a] Male SW Mice were fed either high fat diet or normal diet. On day 60, male SW mice were injected with either STZ (120 mg/kg, ip, in citrate buffer, pH 4.3) or citrate buffer (10 ml/kg, ip). On day 68, type 2 diabetes was confirmed by measuring plasma glucose and insulin levels. On days 69 and 70, the DB (DB + CLC) and non-DB (ND group) mice received colchicine (CLC, 2 mg/kg and 1.5 mg/kg, ip, in distilled water, at 48 and 12 h before APAP administration, respectively), while the other group of DB mice received distilled water (DB + DW, 10 ml/kg, ip, at 48 and 12 h before APAP treatment). On day 71, both the groups DB mice (DB + CLC and DB + DW) were injected with single dose of acetaminophen (APAP, 600 mg/kg, ip, in warm basic saline, pH 8). Also, another group of DB and non-DB (ND group) mice treated with CLC to control for any effects of CLC itself received saline (vehicle for APAP) were maintained. Survival and mortality were observed thrice on the first day and twice daily thereafter for a total of 14 days. Number of deaths and time were recorded.

[b] All deaths occurred between 8 and 24 h after toxicant challenge.

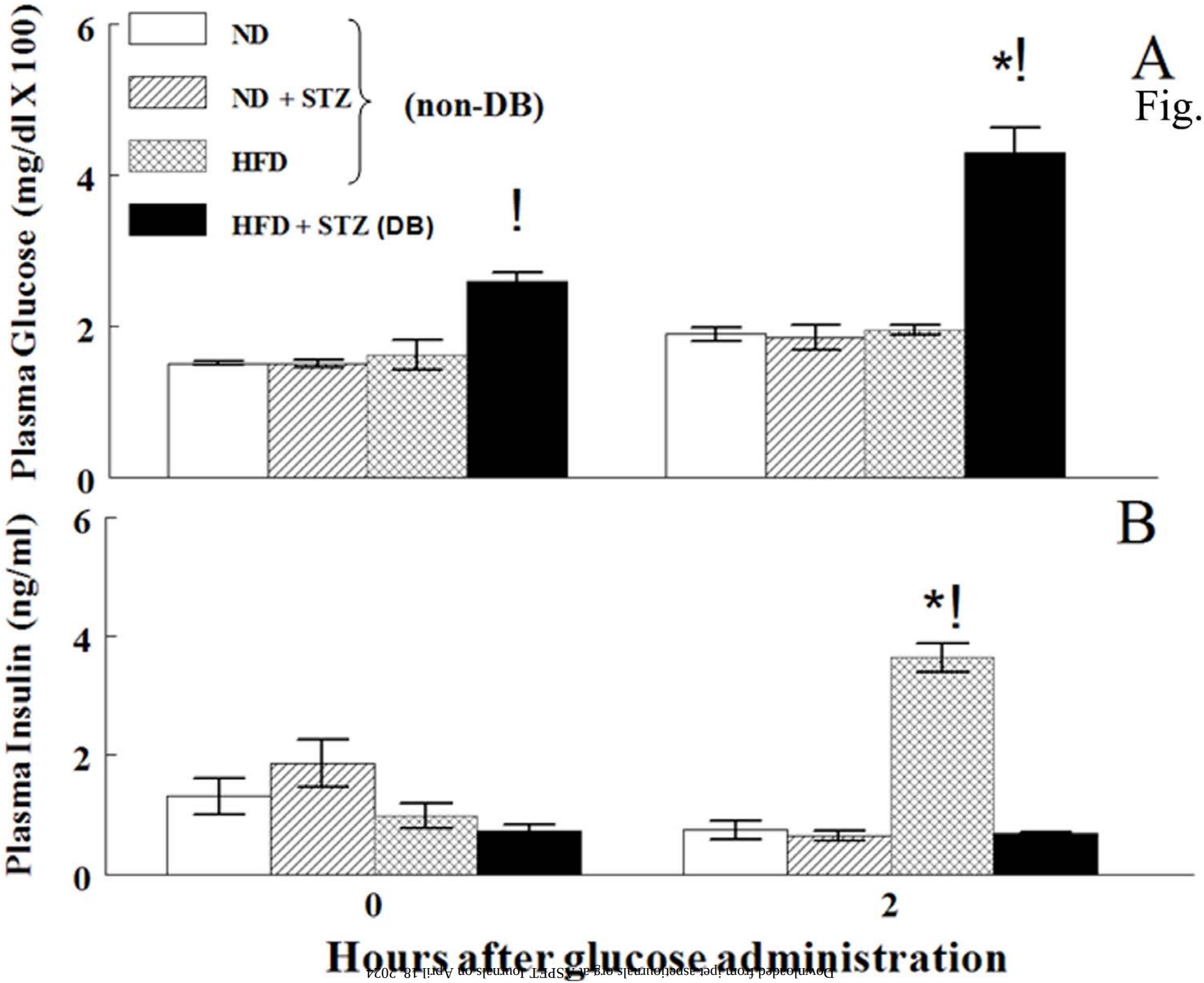

Fig. 1

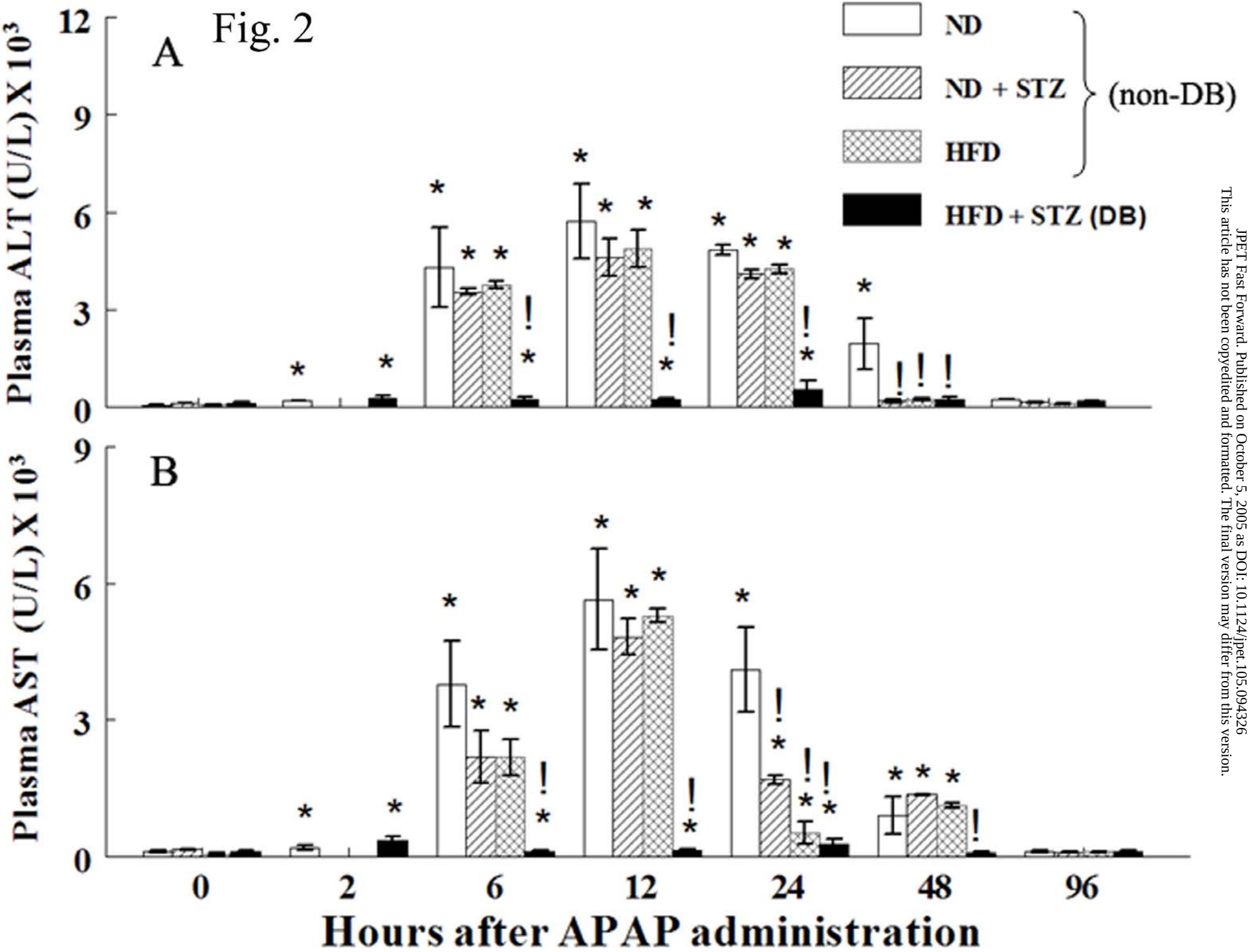

JPET Fast Forward. Published on October 5, 2005 as DOI: 10.1124/jpet.105.094326
This article has not been copyedited and formatted. The final version may differ from this version.

ND (non-DB) DB Fig. 3

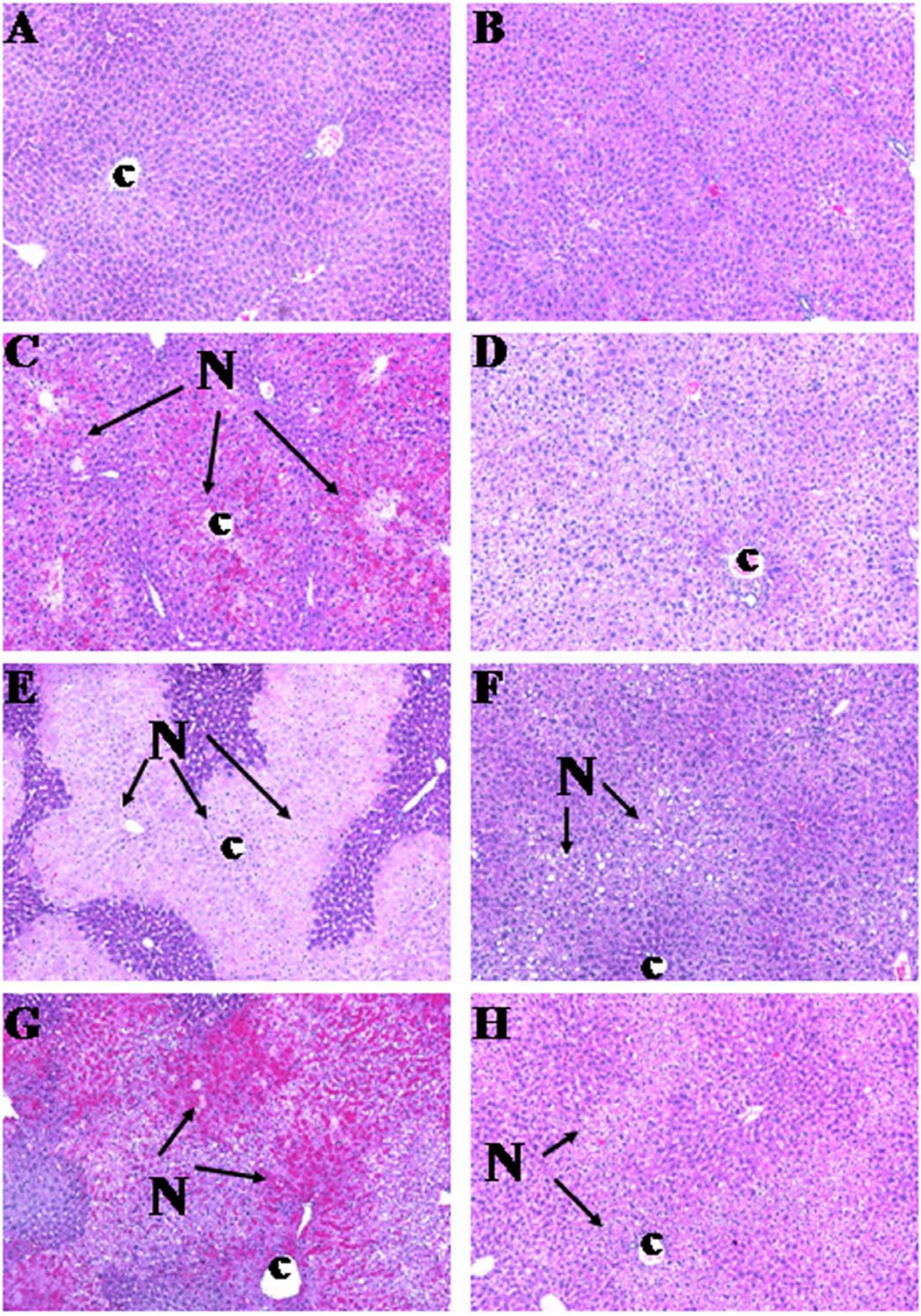

Fig. 4

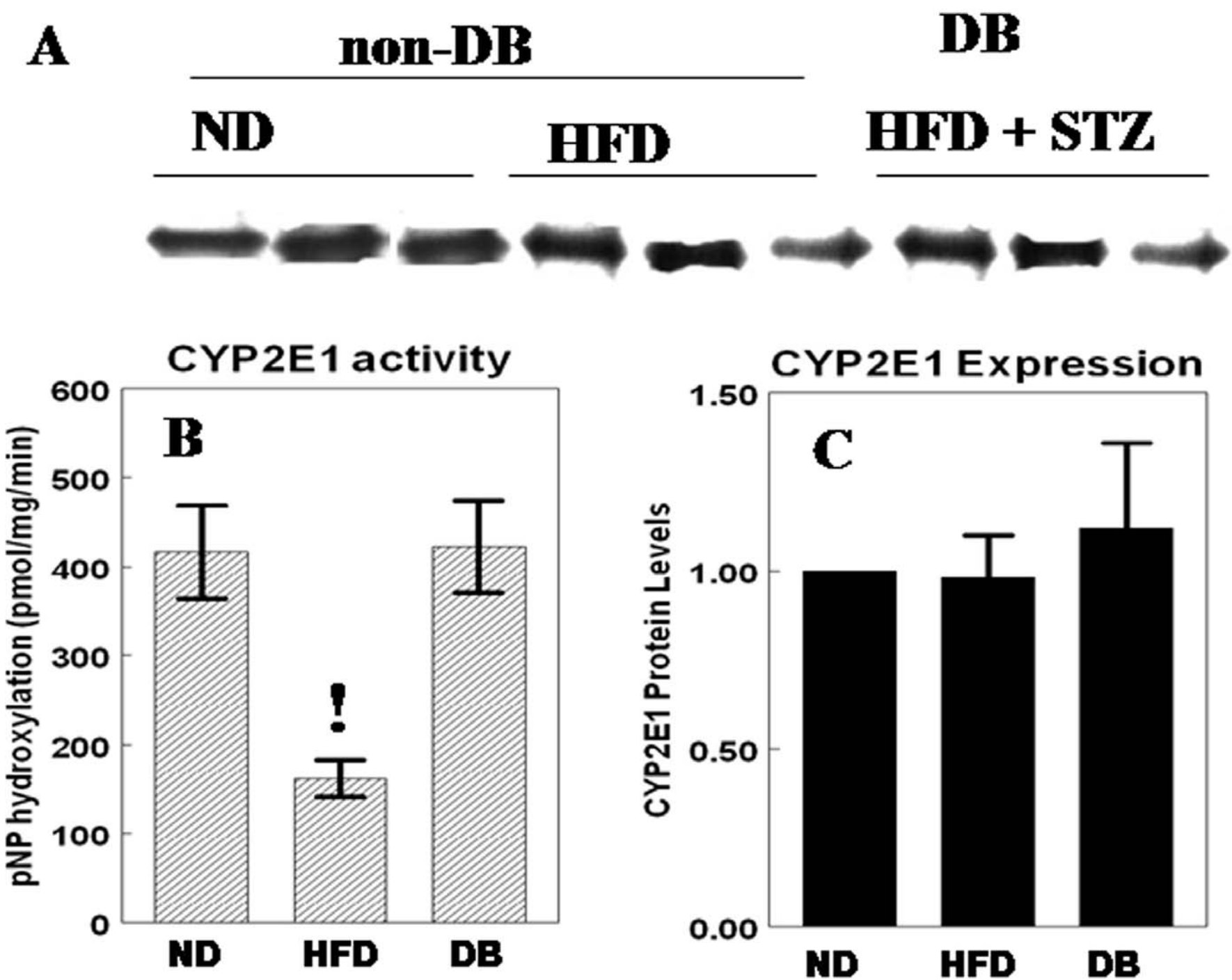

Fig. 5

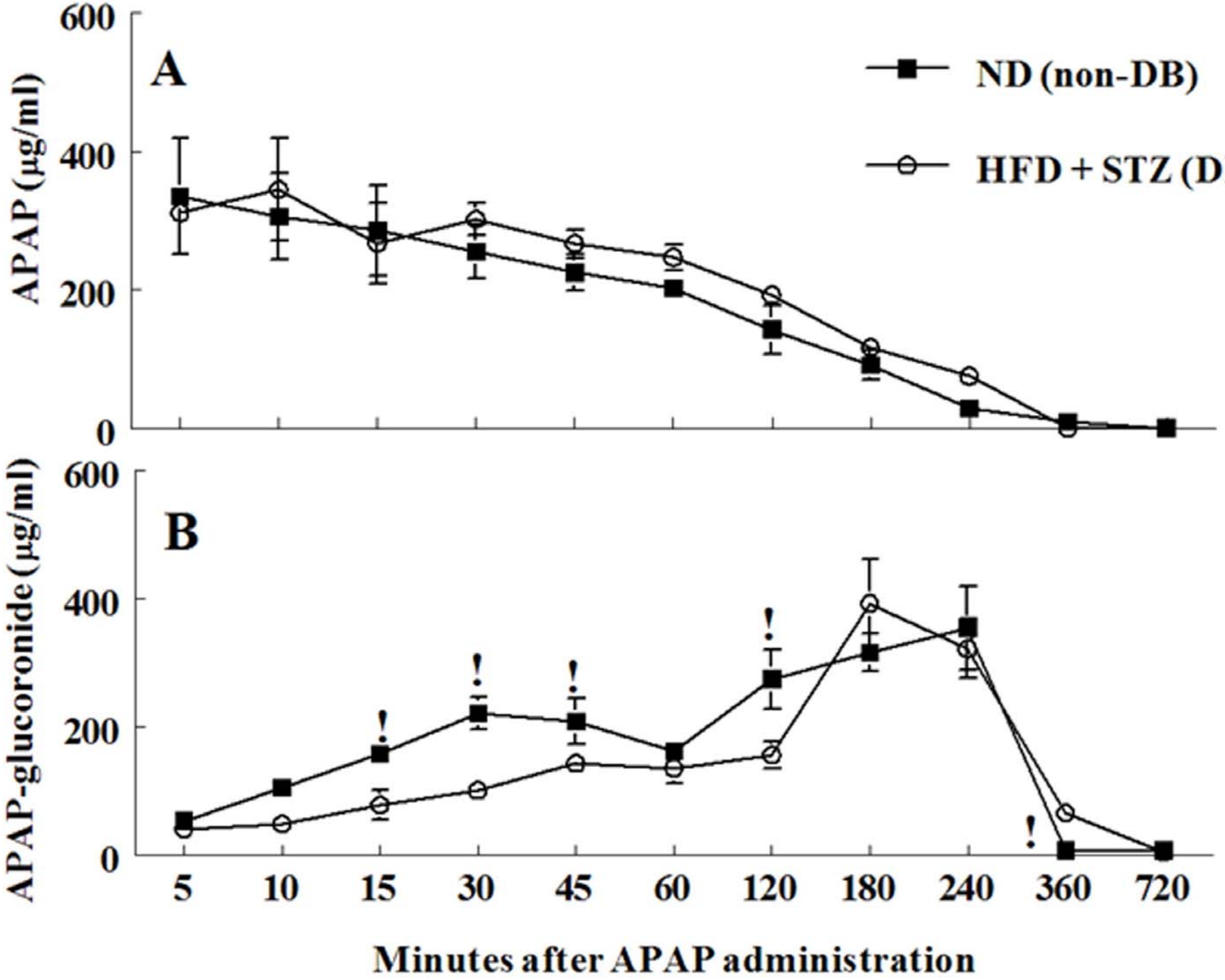

Fig. 6

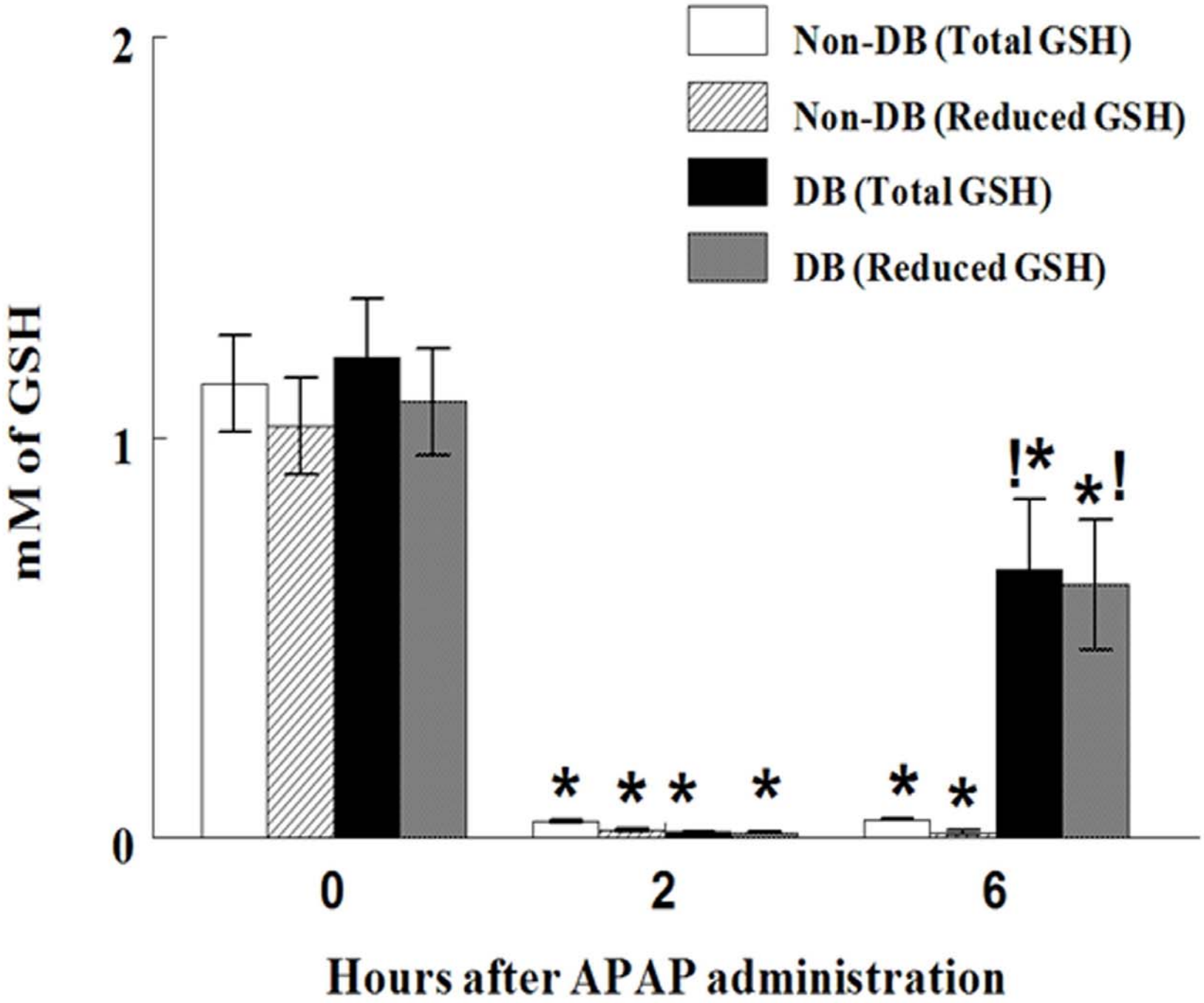

ND (non DB) DB Fig. 7

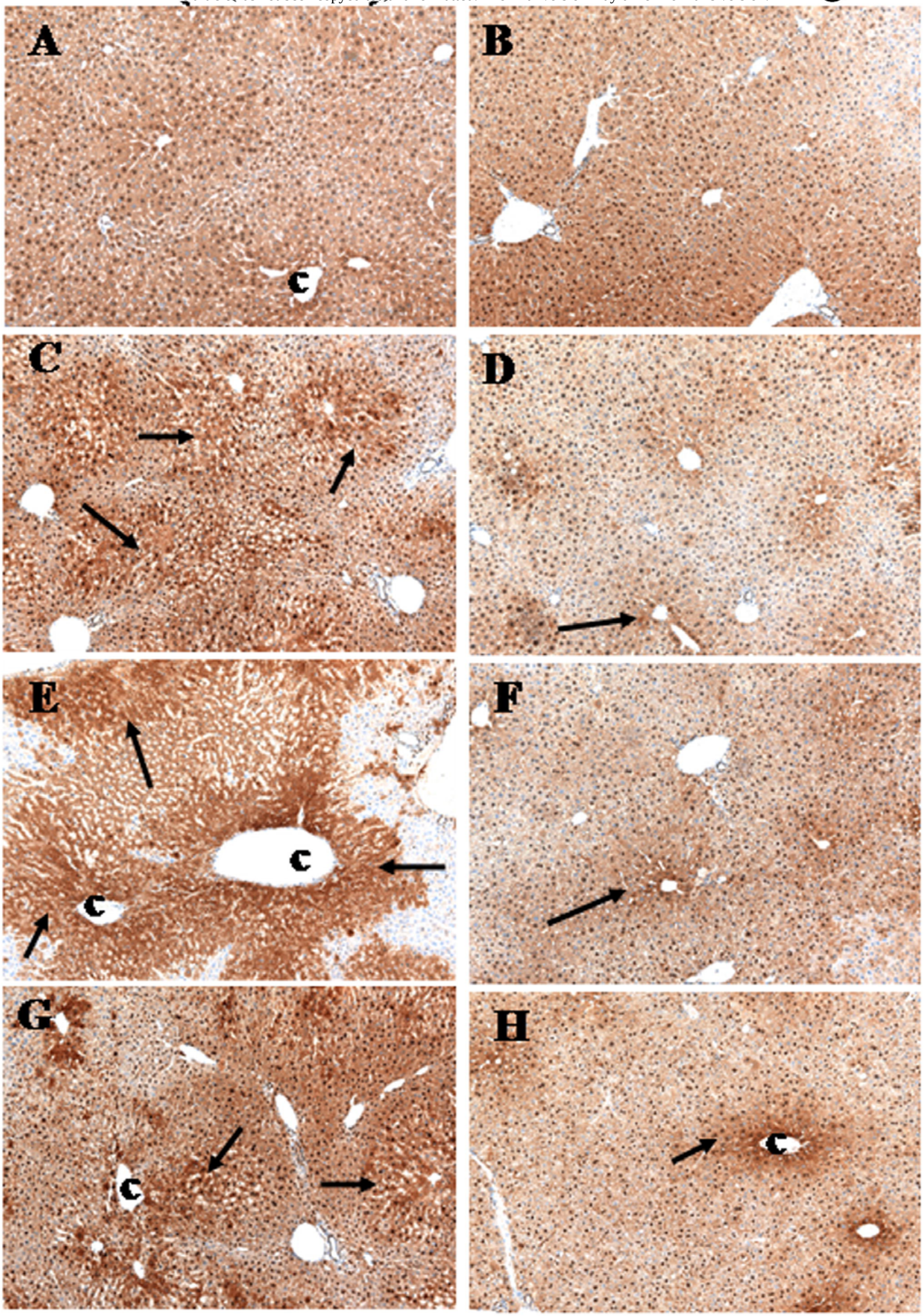

Fig. 8

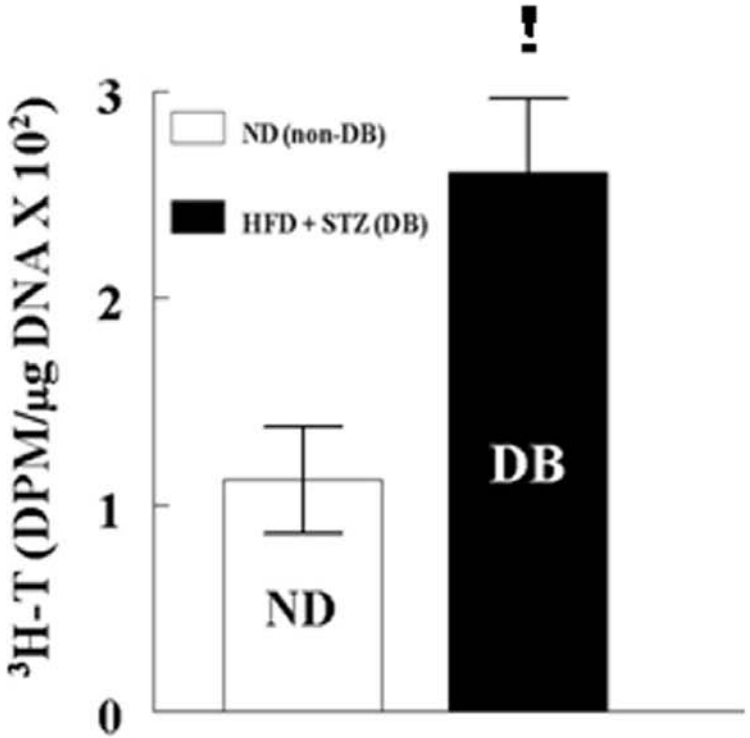

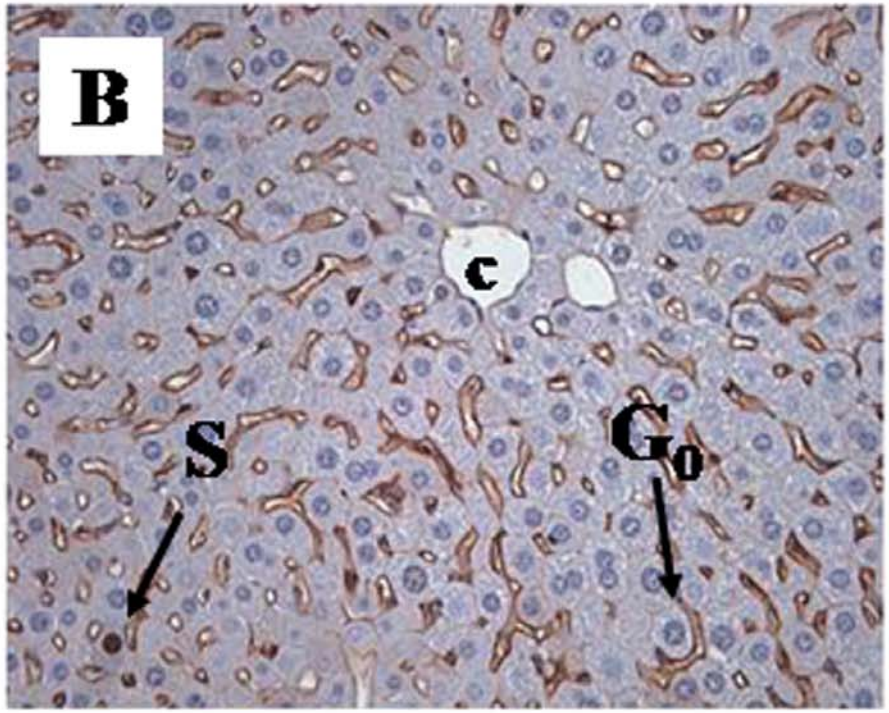

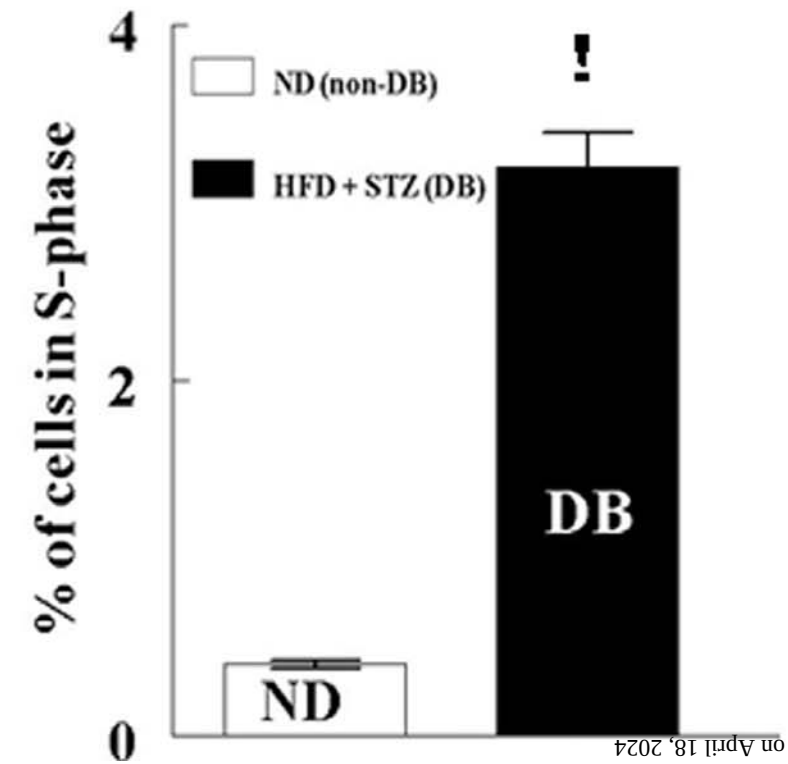

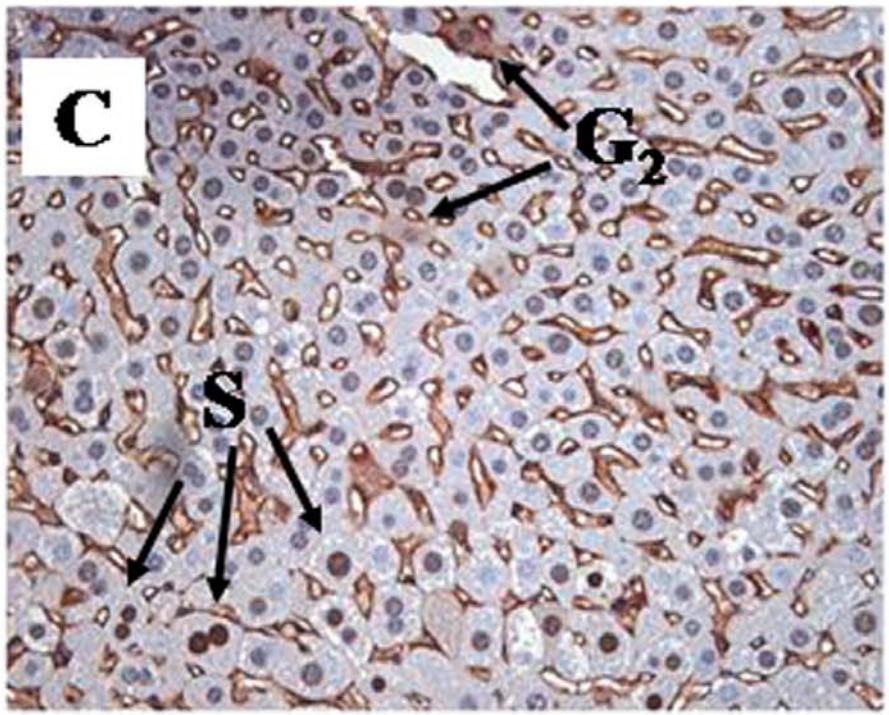

Fig. 9

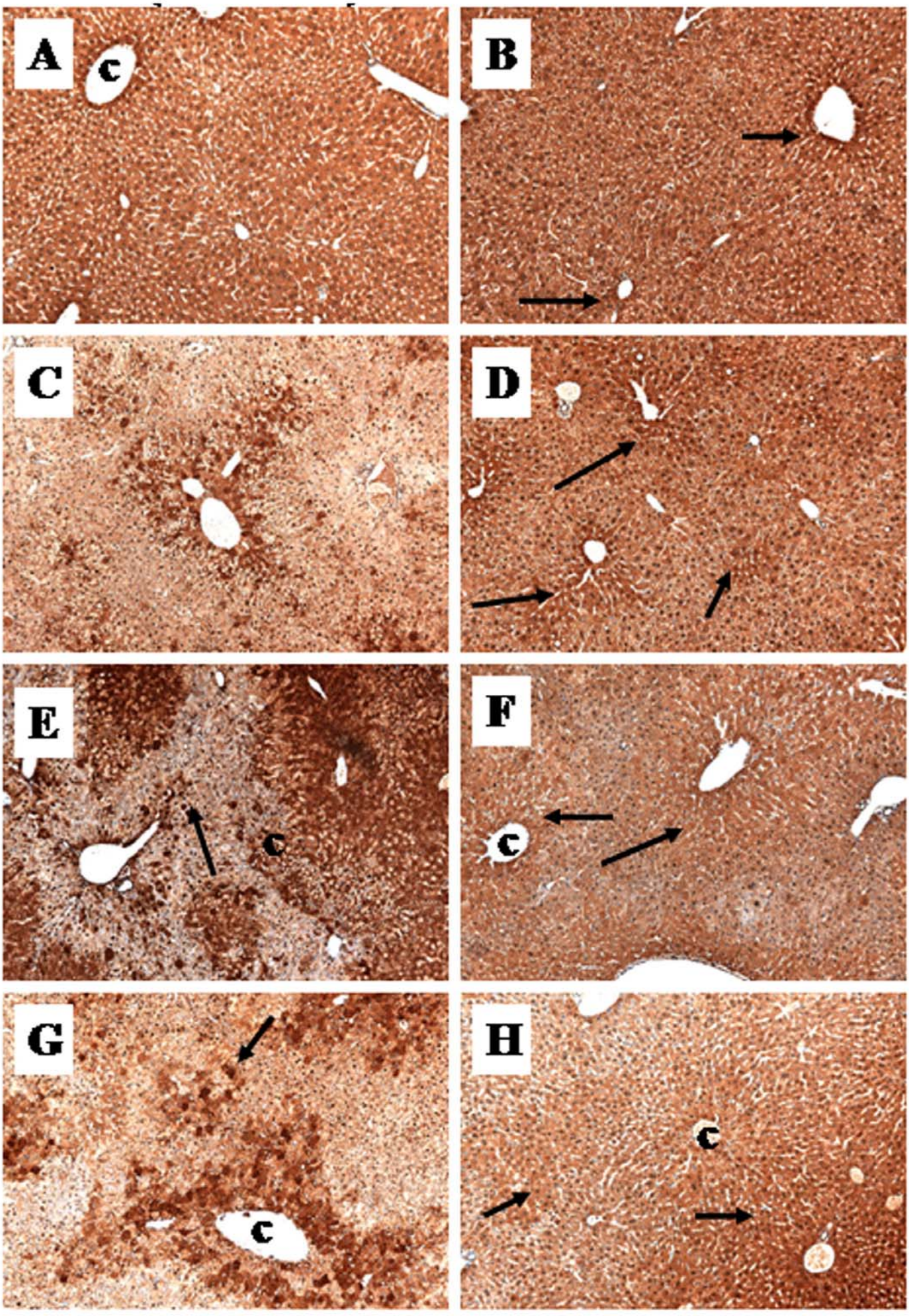

Fig. 10